

Cayley configuration spaces of 2D mechanisms

Part I: extreme points, continuous motion paths and minimal representations

Meera Sitharam, Menghan Wang, Heping Gao

November 5, 2018

Abstract

We consider longstanding questions concerning configuration spaces of *1-degree-of-freedom tree-decomposable linkages* in 2D, an algebraically well-defined class that commonly occurs in mechanical computer aided design. By employing the notion of a *Cayley configuration space*, i.e., a set of intervals of realizable distance-values for an independent non-edge, we answer the following. (1) How to measure the complexity of the configuration space and efficiently compute configuration spaces of low algebraic complexity? (2) How to define realization or orientation types that restrict the Cayley configuration space to be a single interval? (3) How to efficiently obtain continuous motion paths between realizations? (4) How to find a bijective representation of the Cartesian realization space as a curve in an ambient space of minimum dimension? Such a representation would provide an efficient notion of distance between connected components of the realization space (5) How robust is the complexity measure from (1) and how to efficiently classify and characterize linkages according to this complexity measure?

In Part I of this paper, we deal with problems (1)–(4) by introducing the notions of (a) Cayley size, i.e., the number of intervals in the Cayley configuration space, (b) Cayley computational complexity of computing the interval endpoints, as a function of the number of intervals, and (c) Cayley (algebraic) complexity of describing the interval endpoints. Specifically (i) We give an algorithm to determine the interval endpoints of a Cayley configuration space by characterizing the Cartesian realizations corresponding to these endpoints. For graphs with low Cayley (algebraic) complexity, we give the following. (ii) A natural, minimal realization type, i.e. a minimal set of local orientations, whose specification guarantees Cayley size of 1 and $O(|V|^2)$ Cayley computational complexity. Specifying fewer local orientations results in a superpolynomial blow-up of both the Cayley size and computational complexity, provided P is different from NP. (iii) An algorithm—for generic linkages (as defined here)—to find a path of continuous motion (provided one exists) between two given realizations, in time linear in a natural measure of the length of the path. We show that the number of such paths is at most two. (iv) A canonical bijective representation of the Cartesian realization space in minimal ambient dimension, also for generic linkages. We provide a comparison of our results with relevant previous work.

1 Introduction

A *linkage* (G, \bar{l}) , is a graph $G = (V, E)$ with fixed length bars as edges, i.e. $\bar{l} : E \rightarrow \mathbb{R}$. A 2D (Cartesian) *realization* $G(p)$ of G is an assignment of points $p \in \mathbb{R}^2$ to the vertices of G , satisfying the bar lengths in \bar{l} , i.e., for all edges $(u, v) \in G$, $\|p_u - p_v\| = \bar{l}(u, v)$ where $p_u, p_v \in \mathbb{R}^2$. Note that a linkage may or may not have a 2D realization.

We will use standard and well-known terminology from geometric constraint solving and combinatorial rigidity. For detailed background in these fields we refer the reader to, for example, [8] and [20]. The *degrees of freedom (dofs)* of a linkage is the minimum number of new

bars that need to be added in order to ensure that a generic realization of the linkage (with the new bars) is *rigid*, i.e., its bar lengths permit no motions other than the Euclidean or rigid body motions (translations or rotations), otherwise the linkage is *flexible*.

Describing and analyzing realization spaces of 1-dof linkages or *mechanisms* in 2D is a difficult problem with a long history. In mechanical computer aided design, it represents a key underlying barrier to understanding underconstrained geometric constraint system. In fact, even for rigid linkages, the number of realizations can be exponential in the number of vertices and not easy to estimate [1]. One way to classify realizations is to use *realization types* [22, 5], which uniquely determines a realization of a rigid linkage. For flexible linkages, a well-known early result [12] shows that an arbitrary algebraic curve can be traced by the motion of a linkage joint. One outstanding example is the Peaucellier-Lipkin linkage, which transforms planar rotary motion into straight-line motion [13]. For polygonal linkages, recent results on the variants of Carpenter’s rule problem and pseudotriangulations yield spaces of non-crossing realizations and expansive motions [26, 25, 3, 17]. Versions of the problem play an important role in Computer-Aided-Design (CAD), robotics and molecular geometry [18, 28, 20], but few results are known beyond individual or specific families of linkages [11, 27, 7, 29].

There are numerous examples of algorithms and software dealing with 1-dof linkages, such as Geometry Expressions, SAM, Phun, Sketchpad, Geogebra, D-cubed, the algorithm in [9], etc. They have the following major functionalities: (i) designing 1-dof tree-decomposable linkages for tracing out specific curves, especially by building new mechanisms based on a library of existing ones; (ii) accepting user-specified parameters, ranges and realization types to generate continuous motion of the linkages. However, the following issues still exist. (a) Currently, the realization space is typically represented as separate curves in 2D that are traced by each vertex of the linkage. In fact, a realization actually corresponds to a tuple of points, one on each of these curves. I.e., the realization space is bijectively represented by a curve in the full *ambient dimension* of $2|V| - 3$ after factoring out rigid transformations, where $|V|$ is the number of vertices in the linkage. (b) Currently, for two realizations in different connected components, there is no method to find out how “close” they can get towards each other by continuous motion, using a meaningful definition of “distance” between connected components. (c) Currently, in order to generate continuous motion, the user must specify a range of a parameter containing the parameter value at the given realization. Then either a single connected component is generated for a subset of the specified range, or multiple segments of the realization space, under only the given realization type, are generated within the specified range. We discuss this issue in more detail in Section 1.3.

We study the *Cayley configuration space*, first introduced in [6, 21], which is a set of intervals of possible distance-values for an independent non-edge. In both parts of this paper, we restrict ourselves to 1-dof linkages obtained by dropping a bar from minimally rigid, *tree-decomposable linkages*, which are widely used in engineering and CAD, because they are *quadratically-radically solvable* (*QRS*, also called ruler-and-compass realizable), i.e., the realizations are solutions to a triangularized quadratic system with coefficients in \mathbb{Q} (i.e. the solution coordinates belong to an extension field over \mathbb{Q} obtained by nested square-roots).

Let $G = (V, E)$. The graph $G \cup f$, is the graph $(V, E \cup \{f\})$, where the end points of the new edge f are known to be in V . A reasonable way to describe the space of 2D realizations of a 1-dof linkage (G, \bar{l}) is to take a pair of vertices whose distance is not fixed by the bars, i.e., an *independent non-edge* f with $G \cup f$ being minimally rigid, and ask for all the possible lengths l_f that the non-edge f can attain (i) over all the realizations of (G, \bar{l}) ; (ii) over all realizations of (G, \bar{l}) of a particular *T-realization type*. A *T-realization type* of a 2D realization $G(p)$, where T consists of triples of points in p , is a set σ of *local orientations* (chirality) $\sigma_t \in \{+1, -1, 0\}$, each denoting the local orientation of a specific triple of points $t \in T$ (see Definition 3).

For (i) (resp. (ii)), we call each realizable length l_f as a (resp. *T-oriented*) *Cayley configuration*, and the set of all such configurations as the (resp. *T-oriented*) *Cayley configuration space* of the linkage (G, \bar{l}) on f , parameterized by the distance l_f . It is a set of disjoint closed intervals

on the real line. Aside: the Cayley configuration space over f is actually the *projection* of the Cayley-Menger semi-algebraic set [2] associated with the linkage (G, \bar{l}) on the Cayley non-edge length parameter f .

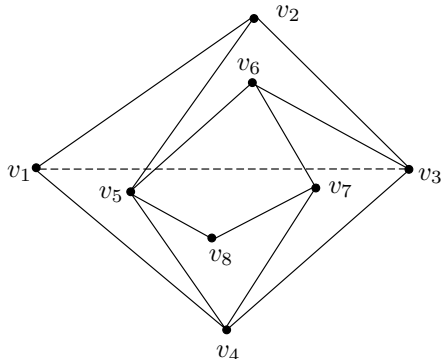


Figure 1: A 1-dof linkage: adding any of the edges (v_i, v_{i+2}) would make the linkage rigid. In Figure 2, we show the Cayley configuration space over the dotted non-edge (v_1, v_3)

For example, the linkage (G, \bar{l}) in Figure 1 is 1-dof, and adding a bar between any of the pairs (v_i, v_{i+2}) would make it rigid. In Figure 2, we choose (v_1, v_3) as the non-edge f of (G, \bar{l}) and give the Cayley configuration space of this linkage over f , consisting of the three intervals shown. It is important to note that Cayley configuration is not always a bijective representation, since each Cayley configuration can (generically) correspond to (finitely) many realizations: the figure shows arbitrarily chosen realizations corresponding to six Cayley configurations. In Figure 3, we take *forward realization types* (a special T-realization type defined in Definition 3) σ of realization (C1) from Figure 2 and τ of realization (C2) from Figure 2, and show the two corresponding *forward-oriented Cayley configuration spaces* of (G, \bar{l}) over f . Each of these oriented Cayley configuration spaces consists of a single interval.

1.1 Questions

In this paper, we consider various natural questions about a well-known class of 1-dof linkages.

- (In Part I) (1) Is there a robust measure of complexity of the Cayley configuration space of a linkage (G, \bar{l}) over f , that depends only on the graph G and the non-edge f , and not on the bar lengths \bar{l} ? (2) How can we obtain a Cayley configuration space? (3) How to define realization of orientation types that restrict the corresponding oriented Cayley configuration space to be a single interval? (4) How can we use a Cayley configuration space to obtain paths of continuous motion between realizations? (5) How to obtain a canonical bijective representation of the Cartesian realization space using minimum ambient dimension?
- (In Part II) (6) Is there a robust measure of complexity for Cayley configuration spaces, that does not even depend on the choice of non-edge f ? (7) Is there a natural characterization and/or efficient algorithmic characterization of graphs G that have Cayley configuration spaces of low complexity?

In order to state our contributions more precisely, in the next section, we define several natural complexity measures for Cayley configuration spaces.

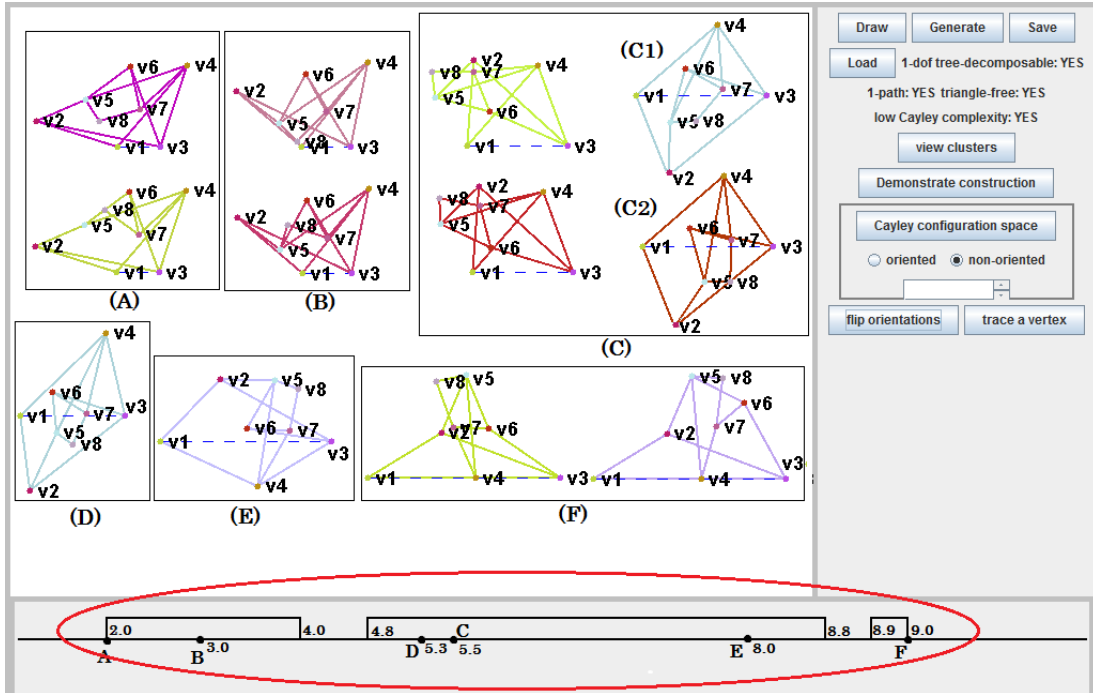


Figure 2: The circled part is the Cayley configuration space of the 1-dof linkage in Figure 1 over $f = (v_1, v_3)$ (demonstrated using our new CayMos software [23]. See also a demonstration video at <http://www.cise.ufl.edu/~menghan/caymos/definitions.avi>.) Each Cayley configuration corresponds to many realizations. Arbitrarily chosen realizations for Cayley configurations: (A) $l_f = 2$, (B) $l_f = 3$, (C) $l_f = 5.5$, (D) $l_f = 5.3$, (E) $l_f = 8$, (F) $l_f = 9$.

1.2 Complexity measures for Cayley configuration spaces

Consider the (oriented) Cayley configuration spaces of 1-dof linkages with underlying graph G over a non-edge f . We take the following as measures of complexity:

- Cayley size* of G , i.e. the maximum number of intervals in the complete description of the (oriented) Cayley configuration space, over all possible linkages (G, \bar{l}) of G .
- Cayley Computational Complexity* of G , the maximum overall time complexity of obtaining the complete (oriented) Cayley configuration space, over all possible linkages (G, \bar{l}) of G . It can be regarded as a function of Cayley size.
- Cayley algebraic complexity* of G , i.e. the maximum algebraic descriptive complexity of each endpoint in the (oriented) Cayley configuration space, over all possible linkages (G, \bar{l}) of G . Specifically, if the bar lengths \bar{l} are in \mathbb{Q} , it is desirable if the endpoints are solutions to a triangularized quadratic system with coefficients in \mathbb{Q} (i.e. the endpoints belong to an extension field over \mathbb{Q} obtained by nested square-roots). Such values are called *quadratically-radically solvable*, or *QRS*.

Before investigating these complexity measures, we discuss two desirable requirements on the Cayley configuration space. First, for each Cayley configuration l_f , there should exist only finitely many (could be exponential in $|G|$) realizations of $(G \cup f, \bar{l})$. This is guaranteed if the linkage $(G \cup f, \bar{l})$ is rigid. Second, with a specified realization type, there should exist a linear time algorithm to convert from a Cayley configuration l_f to a corresponding Cartesian realization. As an example, the linkage in Figure 1 satisfies both requirements when we choose

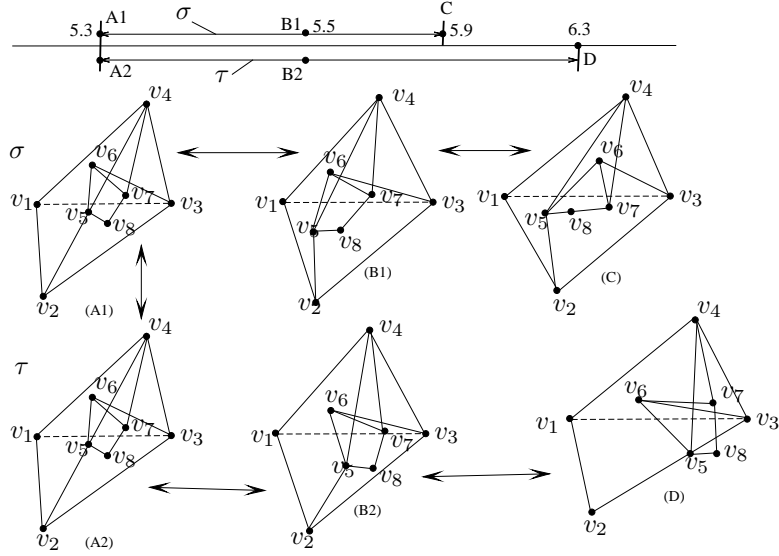


Figure 3: Two oriented Cayley configuration spaces of the 1-dof linkage in Figure 1, and unique realizations for oriented Cayley configurations (A1)(A2) $l_f = 5.3$, (B1)(B2) $l_f = 5.5$ (realizations (C1)(C2) from Figure 2), (C) $l_f = 5.9$, (D) $l_f = 6.3$.

any non-edge $f = (v_i, v_{i+2})$ as the Cayley parameter, since there exists a simple ruler and compass realization of the linkage $(G \cup f, \bar{l})$ from any such f . For linkages with such a realization, the coordinate values of realizations are QRS, and we call such linkages *QRS linkages*, and the underlying graphs *QRS graphs*.

With these two requirements in mind, we focus on a natural class of 1-dof linkages called *1-dof tree-decomposable linkages*. The underlying graphs are obtained by dropping an edge from so-called *tree-decomposable graphs* (formally defined in Section 2). Tree-decomposable graphs are minimally rigid and well-studied, for example, in geometric constraint solving for CAD, because they are QRS [5]. Conversely, QRS has been shown [16] to generically imply tree-decomposability in the case of planar graphs, and the implication is strongly conjectured for all graphs. Our initial example in Figure 1 is a 1-dof tree-decomposable linkage.

1.2.1 Model of Computation

Our complexity measures are based on a model of computation that uses exact representation of numbers in any quadratic extension field of the rational numbers. In other words, we assume that all arithmetic operations, over extraction of square roots and comparison are constant time, exact operations. This model of computation is not as strong as the real RAM model that is normally used in computational geometry, that permits exact representation of arbitrary algebraic numbers [15]. Issues in exact geometric computation such as efficient and robust implementation of such a representation, for example using interval arithmetic, are beyond the scope of this manuscript.

1.3 Contributions and novelty

Contributions of Part I: In Part I we only consider *generic* 1-dof, tree-decomposable linkages. By a *generic* linkage, we mean that no bar length is zero, all bars have distinct lengths and at most one pair of adjacent bars can be collinear in any realization. We answer the following questions posed in Section 1.1.

- (1) How to obtain a Cayley configuration space?

We answer this question by giving two algorithms for obtaining a Cayley configuration space. One algorithm works for any 1-dof tree-decomposable linkage. The other only works for linkages whose underlying graphs have *low Cayley complexity* – i.e. all interval endpoints in the corresponding (oriented) Cayley configuration spaces being tree-decomposable.

- (2) Given a linkage whose underlying graph has low Cayley complexity, can we define realization types whose specification restricts the corresponding oriented Cayley configuration space to be a single interval?

We answer this question by giving a natural *minimal realization type*, i.e. a set of local orientations, whose specification guarantees Cayley size of 1 (i.e., the set of realizable distances for the chosen non-edge is a single interval) and Cayley computational complexity of $O(|V|^2)$. We also show that specifying fewer local orientations than those contained in the minimal realization type results in a superpolynomial blow-up of both the Cayley size and computational complexity, provided P is different from NP .

- (3) From (1) and (2) we can immediately answer the following questions for linkages whose underlying graphs have low Cayley complexity: given two realizations or two Cayley configurations of a linkage, can we determine if there exists a path of continuous motion between them? How do we obtain such a path if it exists? How can we bijectively represent the realization space using minimum ambient dimension?

In our paper, we show that for generic 1-dof tree-decomposable linkages with low Cayley complexity, the path between two realizations is at most two, and can be directly obtained from the oriented Cayley configuration spaces. Provided a path exists, it can be found in time linear in the number of interval endpoints of oriented Cayley configuration spaces that the path contains. Moreover, when the two realizations have the same minimal realization type as in (2) above, it is guaranteed that there exists a path between them staying within the same minimal realization type as these two realizations; and the time complexity of finding that path is $O(1)$. In addition, we give a canonical bijective representation of the realization space in minimal ambient dimension. This representation allows us to meaningfully visualize the realization space, as well as define a canonical distance between different connected components of the realization space.

Contributions of Part II: Part II of the paper answers the following questions from Section 1.1.

Consider the Cayley configuration space of a 1-dof linkage with a underlying graph G over any non-edge f , such that $G \cup f$ is tree-decomposable. Does the Cayley complexity depend on the choice of f ? We answer this question in the negative. Specifically, we show that if the Cayley configuration space over some choice of f has low Cayley complexity, then then the Cayley configuration space over any choice of f also has low Cayley complexity. This shows robustness of the Cayley complexity measure for 1-dof tree-decomposable graphs, and yields an algorithm that runs in time $O(|V|^2)$ to determine low Cayley complexity.

Finally, we answer the question: can we combinatorially characterize 1-dof tree-decomposable graphs G with *low Cayley algebraic complexity*, i.e. all interval endpoints in the corresponding (oriented) Cayley configuration spaces being QRS, without checking every such endpoint? We show a surprising result that (graph) planarity is equivalent to low Cayley algebraic complexity for a natural subclass of 1-dof tree-decomposable graphs. While this is a finite forbidden minor graph characterization of low Cayley algebraic complexity, we provide counterexamples showing impossibility of such finite forbidden minor characterizations when the above subclass is enlarged.

Implementation of the algorithms developed in Part I, Part II and further functionalities is part of our new CayMos software, whose architecture is described in [23] and web-accessible

at <http://www.cise.ufl.edu/~menghan/caymos/>. See also demonstration videos at this website. A different manuscript [24] describes Cayley and Cartesian configuration space analysis and motion analysis of common and well-known mechanisms using CayMos.

1.3.1 Comparison with related work

A key feature of our results is the essential and judicious *interplay between simple algebraic geometry properties* (Part I of this paper) *and simple graph theoretic properties* (Part II of this paper) of these linkages. To the best of our knowledge, the only known result in this area that has a similar flavor of combinatorially capturing algebraic complexity is the result of [16] that relates quadratic solvability and tree-decomposability for planar graphs.

Concerning the use of Cayley parameters or non-edges for parametrizing the configuration space, the papers [11, 20, 29] study how to obtain “completions” of underconstrained graphs G , i.e, a set of non-edges F whose addition makes G minimally rigid. All are motivated by the need to efficiently obtain realizations of flexible linkages. In particular [11] also guarantees that the completion ensures tree-decomposability. However, they do not even attempt to address the question of how to find realizable distance values for the completion edges. Nor do they address algebraic complexity of the set of distance values that these completion non-edges can take, nor the complexity of obtaining a description of this configuration space, nor a combinatorial characterization of graphs for which this complexity is low. The latter factors however are crucial for tractably analyzing and decomposing the realization space in order to obtain the corresponding realizations. On the other hand, the paper [27] gives a collection of useful observations and heuristics for computing the interval endpoints in the configuration space descriptions of certain linkages that arise in real CAD applications, by decomposing the linkages into subproblems. However, it relies on a complete list of solutions for all possible subproblems. Nor does it address the complexity issues mentioned above.

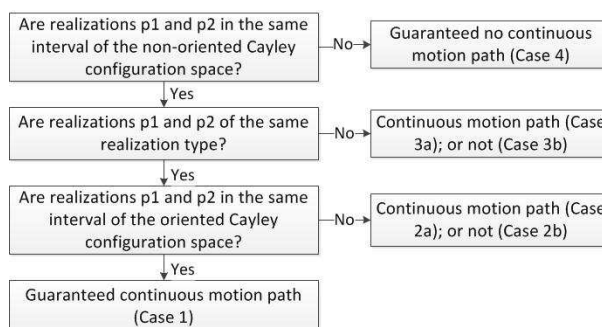


Figure 4: Complete case analysis of continuous motion paths between two realizations p_1 and p_2 .

We know that the Cayley configuration is not always a bijective representation of the realization space. A non-oriented Cayley interval, being a union of multiple oriented Cayley intervals, could correspond to multiple connected components of the realization space, as in Figure 2. Although an oriented Cayley interval corresponds to a unique connected component, the mapping is not bijective, since that same connected component could contain more than one oriented interval. Figure 4 summarizes the different cases when determining existence of a continuous motion path between two realizations. There are two cases (2 and 3) where there may or may not exist a continuous motion path (a and b).

Previous algorithms and software, except for [9], generate continuous motion within a specified Cayley interval, or multiple segments of continuous motion, each corresponding to different oriented Cayley interval with the same realization type. Thus they cannot consistently distinguish Case 2a from Case 2b, or Case 3a from Case 3b. The algorithms in [9] can distinguish

between these four types. However, it deals with general tree-decomposable linkages, relies on exhaustive searching and could have exponential time complexity.

1.4 Organization of Part I

In Section 2, we give basic definitions related to 1-dof tree-decomposable graphs.

In Section 3, we associate a special so-called *extreme graph* with each interval endpoint of a (oriented) Cayley configuration space. We also give the precise definition of low Cayley complexity.

In Section 4, we prove that $O(1)$ Cayley size and $O(|V|^2)$ Cayley computational complexity will be guaranteed when a natural *minimal realization type* – i.e. a minimal set of local orientations – is fixed, for a graph with low Cayley complexity. We also show that specifying fewer local orientations than those contained in the minimal realization type results in a superpolynomial blow-up of both the Cayley size and computational complexity, provided P is different from NP .

In Section 5, we give an algorithm to find a path of continuous motion between two given realizations from the oriented Cayley configuration spaces, and show that there are at most two such paths. We also show that when those two realizations have the same minimal realization type, a path staying within the same minimal realization type can always be found in constant time. In Section 5.1, we give a canonical bijective representation the the realization space, which yields a meaningful visualization of the realization space as curves in an ambient space of minimal dimension.

2 Definitions and basic properties of 1-dof tree-decomposable graphs and linkages

Definition 1. A graph G is *tree-decomposable* if:

- it is a single edge; or
- it can be divided into three *tree-decomposable components*, namely tree-decomposable subgraphs G_1 , G_2 and G_3 , such that $G = G_1 \cup G_2 \cup G_3$, $G_1 \cap G_2 = (\{v_3\}, \emptyset)$, $G_2 \cap G_3 = (\{v_2\}, \emptyset)$ and $G_1 \cap G_3 = (\{v_1\}, \emptyset)$, with v_1 , v_2 and v_3 being distinct vertices (see Figure 5(a)).

A graph G is a *1-dof tree-decomposable graph* if there exists a non-edge f such that $G \cup f$ is tree-decomposable. Such an f is called a *base non-edge* of G and a *base edge* of $G \cup f$.

For example, in Figure 5, a tree-decomposable graph is decomposed into three tree-decomposable components, and G_1 is decomposed into G_{11} , G_{12} and G_{13} .

Note. A 1-dof tree-decomposable graph G can have many base non-edges. That is, G may have non-edges $f' \neq f$ such that both $G \cup f$ and $G \cup f'$ are tree-decomposable graphs. We emphasize that this is different from deleting a different edge h from $G \cup f$, which gives an entirely different 1-dof tree-decomposable graph from G .

Definition 2. Any 1-dof tree-decomposable graph G can be constructed iteratively as follows, starting from a given base non-edge f . At the k^{th} *construction step*, two new maximal tree-decomposable subgraphs T_1 and T_2 sharing a single *step vertex* v_k are appended to the previously constructed graph $G_f(k-1)$: T_1 and T_2 each has exactly one shared vertex, u_k and w_k respectively, with $G_f(k-1)$, where $u_k \neq w_k$ (see Figure 6). Vertices u_k , w_k are called the *base pair of vertices at Step k* . We denote this construction step by $v_k \triangleleft (u_k \in T_1, w_k \in T_2)$, or simply $v_k \triangleleft (u_k, w_k)$. We call these maximal tree-decomposable subgraphs T_i the *clusters* of G . If a vertex v is shared by m distinct clusters, we say $cdeg(v) = m$.

A tree-decomposable graph can be constructed in a similar way from a given base edge.

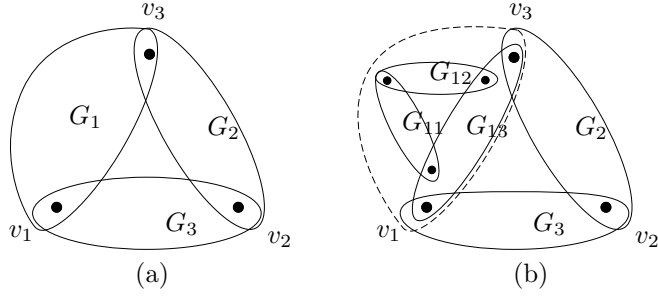


Figure 5: A graph is tree-decomposable if it can be divided into three tree-decomposable components.

For example, refer to Figure 6(a). Construction steps from base non-edge (v_0, v'_0) are: $v_1 \triangleleft (v_0 \in T_1, v'_0 \in T_2)$, $v_2 \triangleleft (v_0 \in T_3, v'_0 \in T_4)$, and $v_3 \triangleleft (u_1 \in T_5, v'_0 \in T_6)$. We have $cdeg(v'_0) = 3$, $cdeg(v_3) = 2$.

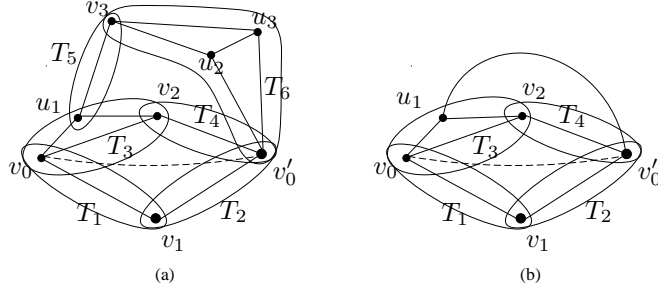


Figure 6: (a) A 1-dof tree-decomposable graph with three construction steps from base non-edge (v_0, v'_0) . (b) The extreme graph of (a) corresponding to the 3^{rd} construction step.

Note. (i) The decomposition of a 1-dof tree-decomposable graph G into clusters is unique [4]. (ii) It follows from the definition that for any construction step $v_k \triangleleft (u_k, w_k)$, the base pair of vertices u_k and w_k must lie in two different clusters T_u and T_w in $G_f(k-1)$. We call T_u and T_w the *base pair of clusters* at Step k .

A linkage (G, \bar{l}) with a 1-dof tree-decomposable underlying graph G generically has one degree of freedom, and a Cayley configuration space with parameter f . Given l_f , the graph construction of $G \cup f$ from f clearly yields a QRS realization sequence of $(G \cup f, \bar{l} \cup l_f)$ from f , where $\bar{l} \cup l_f : E \cup f \rightarrow \mathbb{R}$. Specifically, for each construction step $v \triangleleft (u, w)$, given p_u, p_w and the lengths $\bar{l}(v, u)$, $\bar{l}(v, w)$, p_v can be determined by a corresponding simple ruler and compass algebraic solution. The realization may not be unique, since for each realization step we may have two possible *local orientations*.

Definition 3. A construction step $v \triangleleft (u, w)$ of a 1-dof tree-decomposable graph G can be associated with a *local orientation* for the corresponding realization step of a linkage (G, \bar{l}) . This local orientation σ_k takes a value in $\{+1, -1, 0\}$, which represents the sign of the determinant

$$\Delta = \begin{vmatrix} p_w - p_u \\ p_v - p_u \end{vmatrix}$$
. A *forward realization type* is a T -realization type, where T is the set of triples of points corresponding to vertices (v, u, w) , where $v \triangleleft (u, w)$ represent the construction steps of G from f . A *forward-oriented Cayley configuration space* is a T -oriented Cayley configuration space with respect to forward realization type.

Note. In the following discussion, when referring to oriented Cayley configuration spaces of 1-

dof tree-decomposable graphs, unless otherwise specified, we always mean the forward-oriented Cayley configuration spaces.

For example, refer to Figure 7 (a) and (b). The graph is 1-dof tree-decomposable with base non-edge $f = (v_0, v'_0)$. The realization step $v_3 \triangleleft (v_1, v_2)$ can choose from two possible local orientations: (a) has $\sigma_3 < 0$, while (b) has $\sigma_3 > 0$ by flipping v_3 to the other side of (v_1, v_2) .

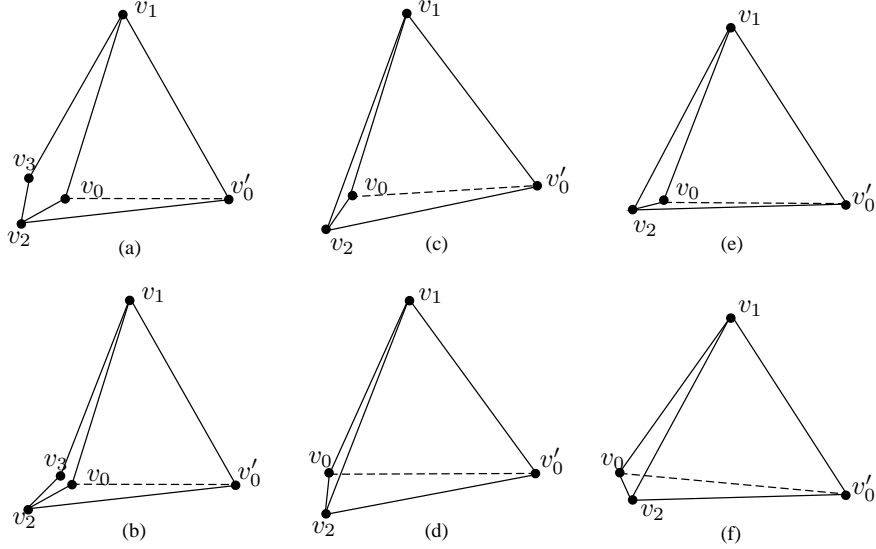


Figure 7: (a) (b): Two choices exist for local orientation of realization step $v_3 \triangleleft (v_1, v_2)$ from base non-edge $f = (v_0, v'_0)$. (c) (d): realizations for extreme linkage $(\hat{G}_f(3), \bar{l}^{\max})$. (e) (f): realizations for extreme linkage $(\hat{G}_f(3), \bar{l}^{\min})$.

Remark 1. Since the total number of forward realization types is exponential in the number of construction steps, only by knowing the forward realization type can we guarantee linear time complexity for realizing a tree-decomposable linkage, i.e., for obtaining a realization from a Cayley configuration of a 1-dof tree-decomposable linkage.

A video demonstrating the basic definitions of 1-dof tree-decomposable linkages and Cayley configuration spaces can be found at <http://www.cise.ufl.edu/~menghan/caymos/definitions.avi>.

3 Extreme graphs and interval endpoints of Cayley configuration space

We use the notion of *extreme graphs* and *extreme linkages* to describe the endpoints of the Cayley configuration space of a 1-dof tree-decomposable linkage (G, \bar{l}) over f .

Definition 4. The k^{th} *extreme graph* for f of a 1-dof tree-decomposable graph G , where the k^{th} construction step of G from f is $v_k \triangleleft (u_k, w_k)$, is the graph obtained by adding a new edge $e_k = (u_k, w_k)$ in $G_f(k-1)$. We denote this extreme graph by $\hat{G}_f(k)$. We call (u_k, w_k) the *extreme edge* of the extreme graph $\hat{G}_f(k)$, and an *extreme non-edge* of G .

Note. It is easy to verify using Laman's theorem [14] that any extreme graph of a 1-dof tree-decomposable graph is minimally rigid.

For example, refer to Figure 6. The 3^{rd} construction step in (a) is $v_3 \triangleleft (u_1, v'_0)$. Connecting $e_3 = (u_1, v'_0)$ in $G_f(2)$, we get the extreme graph $\hat{G}_f(3) = G_f(2) \cup e_3$ in (b).

Definition 5. For a 1-dof tree-decomposable linkage (G, \bar{l}) , the k^{th} extreme linkages are $(\hat{G}_f(k), \bar{l}^{\min})$ and $(\hat{G}_f(k), \bar{l}^{\max})$, where min and max represent the two possible extreme extensions of \bar{l} for the extreme edge $e_k = (u, w)$, obtained from triangle inequalities: $\bar{l}^{\min}(e_k) := |\bar{l}(u, v_k) - \bar{l}(v_k, w)|$, $\bar{l}^{\max}(e_k) := \bar{l}(u, v_k) + \bar{l}(v_k, w)$.

Note. In realizations of $(\hat{G}_f(k), \bar{l}^{\min})$ and $(\hat{G}_f(k), \bar{l}^{\max})$, the local orientation $\sigma_k = 0$. These realizations are sometimes called *unyielding* realizations.

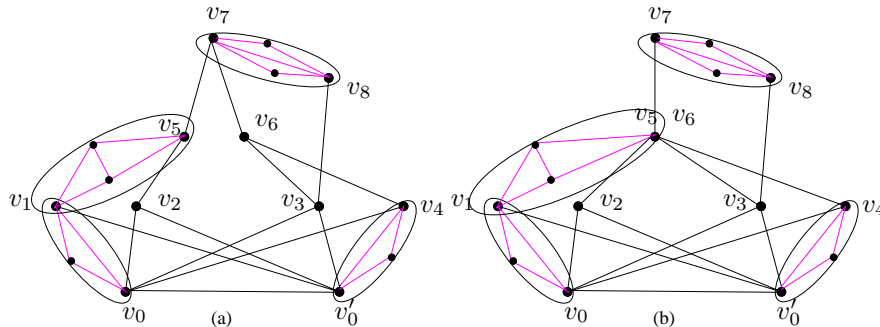


Figure 8: Example showing the importance of genericity: when $p(v_5)$ and $p(v_6)$ are coincident, $l(v_5, v_8)$ is not a function of $l(v_0, v'_0)$.

The next theorem associates a linkage realization with each endpoint of an (oriented) Cayley configuration space. Note that if (G, \bar{l}) is generic, then for a given Cayley configuration l_f and forward realization type σ , there exists at most one 2D realization: as demonstrated in Figure 8, for any vertex v of G , the point p_v is not unique only if for v 's realization step $v \triangleleft (u, w)$, p_u and p_w are coincident and $\bar{l}(v, u) = \bar{l}(v, w)$.

Theorem 1 (structure of Cayley configuration space). *For a generic 1-dof tree-decomposable linkage (G, \bar{l}) with base non-edge $f = (v_0, v'_0)$, the following hold:*

1. *The (oriented) Cayley configuration space over f is a set of disjoint closed real intervals or empty.*
2. *Any interval endpoint in the (oriented) Cayley configuration space corresponds to the length of f in a realization of an extreme linkage.*
3. *For any vertex v , p_v is a continuous function of l_f on each closed interval of the oriented Cayley configuration space. Consequently, for any non-edge (u, w) , $l(u, w)$ is a continuous function of l_f on each closed interval of the oriented Cayley configuration space.*

Remark 2. While Theorem 1 (2) states that every endpoint of the unoriented Cayley configuration space corresponds to an extreme linkage, the converse is not true. As an example, refer to Figure 2. Realization (D) is an extreme linkage, but it is not an endpoint in the unoriented Cayley configuration space. However we will see in Lemma 4 that the converse is true for oriented Cayley configuration spaces.

The proof of Theorem 1 follows from elementary algebraic geometry and can be considered folklore. However, for completeness, a proof is provided in Appendix A.

Observation 1. (i) *Theorem 1 gives a straightforward algorithm called ELR (extreme linkage realization) to obtain the (oriented) Cayley configuration space for a generic 1-dof tree-decomposable linkage (G, \bar{l}) . The algorithm could take time exponential in the Cayley size.*

(ii) Deciding whether the Cayley configuration space over f is non-empty is a NP-hard problem, and the Cayley computational complexity is superpolynomial unless $P = NP$.

Proof. (i) The ELR algorithm works by realizing all the extreme linkages for f consistent with each forward realization type. Note that since the extreme graphs may not be QRS, realizing each extreme linkage can take time exponential in $|V|$ (requiring the solution of a general multi-variable system of quadratic equations). Additionally, the overall time complexity could be exponential in the actual Cayley size, since many candidate endpoints generated during this procedure could finally lead to dead ends. The detailed version of this algorithm is in Appendix B.

(ii) The problem of determining the existence of a realization of a tree-decomposable linkage is NP-complete by early results [19]. This problem can be reduced to our problem of finding the Cayley configuration space over f , whose decision version is whether the Cayley configuration space is non-empty. Clearly, a realization exists if and only if the Cayley configuration space is not empty. Therefore, the problem of finding the Cayley configuration space over f is NP-hard, and the Cayley computational complexity is superpolynomial unless $P = NP$. \square

By Theorem 1, we can obtain a specific measure of Cayley complexity in terms of extreme graphs. Given the promise that there exists a realization of (G, \bar{l}) corresponding to a specific extreme linkage consistent with a given forward realization type, we now consider the following question: what is the algebraic complexity of l_f , a potential endpoint of the Cayley configuration space? I.e., what is the Cayley complexity of G on f ? The answer depends on whether the extreme graph is QRS or not. If it is not QRS, not only would this adversely affect the Cayley complexity, the Cayley computational complexity could also be exponential in $|V|$ (solving general quadratic systems).

Definition 6. A 1-dof tree-decomposable G is said to have *low Cayley algebraic complexity* on base non-edge f if all extreme graphs of G for f are QRS. Since tree-decomposable graphs are an example of QRS graphs, a 1-dof tree-decomposable G is said to have *low Cayley complexity* on base non-edge f if all extreme graphs of G for f are tree-decomposable.

Note that for planar graphs, QRS and tree-decomposability have been shown [10] to be equivalent, and the equivalence has been strongly conjectured for all graphs.

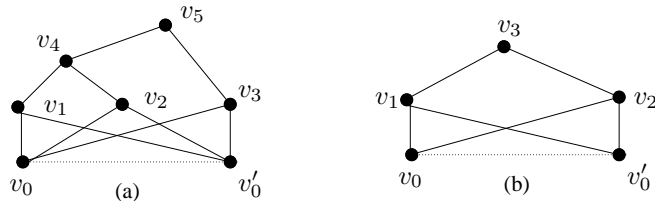


Figure 9: The graph in (b) has low Cayley complexity on (v_0, v'_0) , while the graph in (a) does not.

For example, refer to Figure 9. The graph in (b) has low Cayley complexity on (v_0, v'_0) , while the graph in (a) does not, since the extreme graph corresponding to the construction step of v_5 is not tree-decomposable. We can also verify that the 1-dof tree-decomposable graphs in Figure 1, Figure 6 and Figure 7 have low Cayley complexity on the given base non-edge, while the graph in Figure 8 does not.

4 Finding Cayley configuration spaces for linkages with low Cayley complexity

Suppose we are given a 1-dof tree-decomposable graph G with low Cayley complexity. For any corresponding linkage (G, \bar{l}) , each interval endpoint in its Cayley configuration spaces can be computed essentially using a sequence of solutions of one quadratic equation at a time. We may ask: are we also guaranteed to have small Cayley size and low Cayley computational complexity even for the oriented Cayley configuration spaces? The answer is yes only for a fixed *minimal realization type* (defined below, which is more restrictive than the forward realization type).

Definition 7. For a graph G with low Cayley complexity on f , each extreme graph $\hat{G}_f(k)$ can be constructed with the extreme edge e_k as base edge. We call this a *reverse construction*. Each realization of (G, \bar{l}) corresponds to a *reverse realization type*, a sequence of local orientations for each reverse realization step. A *minimal realization type* consists of both a forward realization type and a reverse realization type.

For example, for the linkage in Figure 7, realizations in (a) and (b) have different forward realization types (thus different minimal realization types). Moreover, since the underlying graph has low Cayley complexity on base non-edge $f = (v_0, v'_0)$, the extreme graph $\hat{G}_f(3)$ has reverse construction $v_0 \triangleleft (v_1, v_2)$, $v'_0 \triangleleft (v_1, v_2)$, where (c)(e) and (d)(f) correspond to different reverse realization types (thus different minimal realization types): (c)(e) have v_0 and v'_0 on the same side of (v_1, v_2) , while (d)(f) have them on opposite sides of (v_1, v_2) .

Observation 1 can be extended to show that in order to guarantee small Cayley size and computational complexity, we need to specify the minimal realization type.

Observation 2. For a 1-dof tree-decomposable graph G with low Cayley complexity on a non-edge f , when the reverse realization type is specified but the forward realization type is unspecified, resp. when the forward realization type is specified but the reverse realization type is unspecified, the problem of obtaining the complete description of Cayley configuration space (decomposition of the Cayley configuration space into a union of oriented Cayley configuration spaces) of a linkage (G, \bar{l}) over f can take time exponential in $|V|$.

Proof. When the reverse realization type is unspecified, the Cayley size can be exponential in $|V|$. Symmetrically, when the forward realization type is unspecified, the number of non-empty oriented Cayley configuration spaces can be exponential in $|V|$. In Appendix C, we use our initial example, the linkage in Figure 1 to demonstrate this exponential blow-up in Cayley size and computational complexity. Existing examples [1] can also be adapted to show the exponential blow-up. Therefore, in both cases, obtaining the decomposition of the Cayley configuration space into a union of oriented Cayley configuration spaces takes time exponential in $|V|$. \square

On the other hand, when the minimal realization type is fixed, for graphs with low Cayley complexity, we show below that the Cayley size is $O(1)$ and the computational complexity is $O(|V|^2)$.

4.1 Finding Cayley configuration spaces when the minimal realization type is fixed

Theorem 2 (fixed minimal realization type). For a 1-dof tree-decomposable graph with low Cayley complexity on a non-edge f , if the minimal realization type is fixed, then the Cayley size is $O(1)$ and the Cayley computational complexity is $O(|V|^2)$.

Idea of the Proof. We first prove the theorem for a special subclass of graphs called *1-path* graphs. Informally, these tree-decomposable graphs have a linearly ordered construction

sequence in a well-defined sense (Definition 9). In the case of general tree-decomposable graphs, this linear order generalizes to a partial order. The proof for 1-path graphs will serve as induction basis for the general case. For the proof of the 1-path case, we utilize Lemma 4 from Part II (Recursive Structure Lemma) concerning the structure of 1-path graphs with low Cayley complexity. Based on this lemma, we obtain a *quadrilateral interval mapping (QIM)* algorithm that correctly finds the Cayley configuration space (Lemma 1, 2), yielding the proof for the 1-path case (Proposition 1).

Next, we prove the multi-path case, by doing induction on the number of *paths* of the graph. This gives a generalization of the QIM algorithm, which however works only when the minimal realization type is fixed (Lemma 3). From this algorithm, we get the proof of the main theorem.

The structure of the proof is schematically shown in Figure 10.

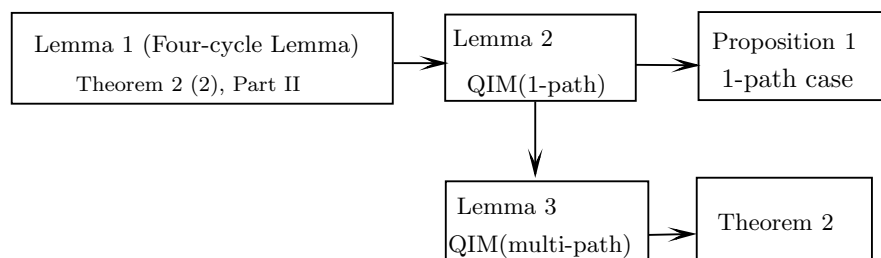


Figure 10: Structure of proof of Theorem 2

We first give the definition of *1-path* graphs.

Definition 8. Given a 1-dof tree-decomposable graph G , a vertex v is in G 's *last level* L_t if: (a) $cdeg(v) = 2$, i.e. there are exactly two clusters T_1 and T_2 sharing v ; (b) each of T_1 and T_2 has only one shared vertex with the rest of the graph $G' = G \setminus (T_1 \cup T_2) = G \setminus \{v\}$.

Definition 9. A 1-dof tree-decomposable graph G has a *1-path construction* from base non-edge $f = (v_0, v'_0)$ if there is only one vertex v in the last level L_t , other than possibly v_0 and v'_0 . As long as there exists a base non-edge permitting 1-path construction, we say the 1-dof tree-decomposable graph G is a *1-path graph*. See Figure 11 for an example.

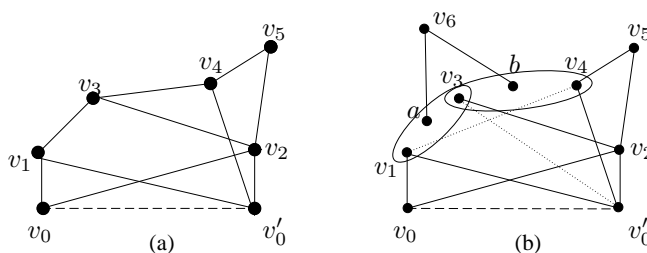


Figure 11: (a) A 1-path graph with v_5 in the last level L_t . (b) A multi-path graph.

The following lemma from Part II gives a key structural property of 1-path, 1-dof, tree-decomposable graphs with low Cayley complexity.

Definition 10 (Definition 3 from Part II). A *four-cycle* of clusters consists of four clusters T_1, T_2, T_3, T_4 such that each consecutive pair has exactly one shared vertex. In other words, we have $T_1 \cap T_2 = \{v_1\}$, $T_2 \cap T_3 = \{v_2\}$, $T_3 \cap T_4 = \{v_3\}$, $T_4 \cap T_1 = \{v_4\}$, where v_1, v_2, v_3, v_4 are distinct vertices. Vertices pairs (v_1, v_3) and (v_2, v_4) are called the *diagonal pairs* of the

four-cycle. For any other vertices u_i, u_{i+1} belonging to adjacent clusters T_i, T_{i+1} , (u_i, u_{i+1}) is called a *chordal pairs* of the four-cycle.

Lemma 1 (Four-cycle Lemma, Theorem 2 (2) from Part II). *Let G be a 1-path tree-decomposable graph with low Cayley complexity on f . For any two distinct base pairs of vertices that we encounter consecutively in the construction of G from f , there exists a four-cycle of clusters such that:*

- (a) *The two consecutive base pairs are the two diagonal pairs of the four-cycle, or:*
- (b) *One base pair is a diagonal pair of the four-cycle, while the other base pair is a chordal pair of the four-cycle.*

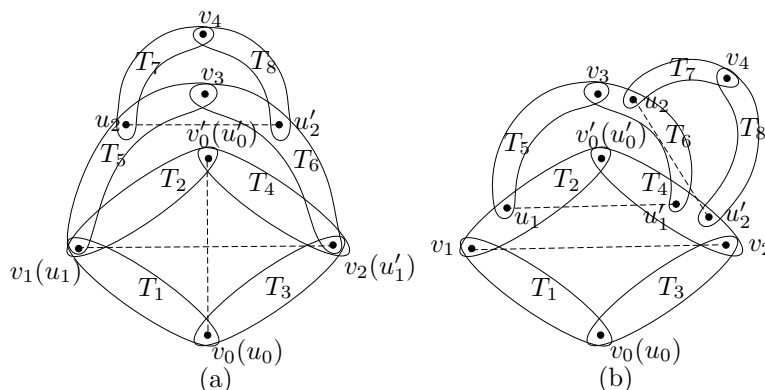


Figure 12: (a) the two pairs (u_1, u'_1) and (u_2, u'_2) shows Case (a) of Lemma 1. (b) the two pairs (u_1, u'_1) and (u_2, u'_2) shows Case (b) of Lemma 1.

4.1.1 The Quadrilateral Interval Mapping (QIM) algorithm

From Lemma 1, we obtain a *quadrilateral interval mapping* (QIM) algorithm for finding the Cayley configuration space over f . We will see the advantage of the QIM algorithm over the ELR algorithm (described in Section 3): only by using the QIM algorithm can we attain linear Cayley computational complexity for 1-path graphs of low Cayley complexity, when the minimal realization type is fixed.

Idea of the QIM algorithm. Consider a quadrilateral with four sides s_1, s_2, s_3, s_4 and two diagonals e_1, e_2 . Since the linkage lives in \mathbb{R}^2 , the volume of the tetrahedron formed by $\{s_1, s_2, s_3, s_4, e_1, e_2\}$ must equal zero. If we know lengths $l(s_1), l(s_2), l(s_3), l(s_4)$, we can get from the volume equation (a so-called Cayley-Menger determinant) an implicit ellipse \mathcal{C} relating attainable $l(e_1)$ and $l(e_2)$ values. See Figure 13 (a). So from the attainable interval $[l^l(e_1), l^r(e_1)]$ of one diagonal e_1 , we can obtain the attainable intervals of $l(e_2)$ by mapping $[l^l(e_1), l^r(e_1)]$ on the curve \mathcal{C} , and vice versa.

The curve \mathcal{C} used in the algorithm has the following useful properties: (1) one specific value of $l(e_1)$ can map to up to 2 distinct corresponding values of $l(e_2)$. Figure 13 (b)(c)(d) illustrates several cases in determining the interval for $l(e_2)$ from $[l^l(e_1), l^r(e_1)]$. This mapping can take a set of intervals for $l(e_1)$ into double the number of intervals for $l(e_2)$. (2) the overall maximum and minimum points of the curve, $p_{\min}(e_1), p_{\min}(e_2), p_{\max}(e_1)$ and $p_{\max}(e_2)$, each corresponds to a change in the minimal realization type. For example, the upper left segment of \mathcal{C} , from $p_{\min}(e_2)$ to $p_{\max}(e_1)$, corresponds to the realization type that the vertices of e_1 lie on different sides of the line specified by e_2 , and the vertices of e_2 lie on the same side of the line specified by e_1 .

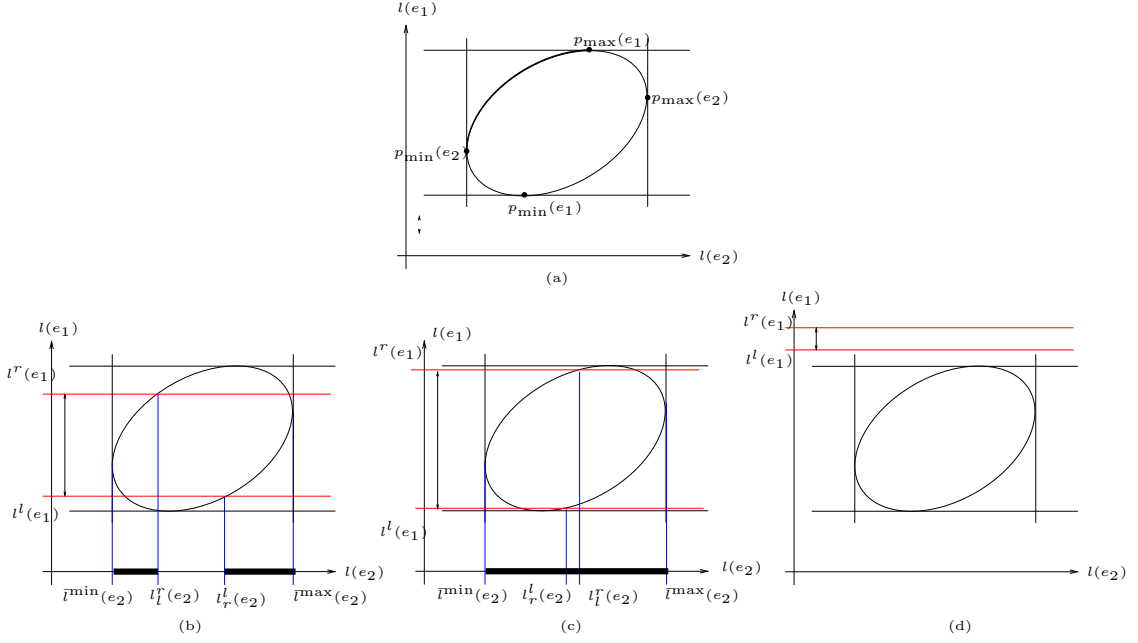


Figure 13: (a) an example of ellipse \mathcal{C} used in QIM; (b)(c)(d) various cases when mapping with ellipse \mathcal{C}

Algorithm (QIM): given a linkage (G, \bar{l}) , where G is a 1-path graph with low Cayley complexity on base non-edge f , we start from the interval $[\bar{l}^{\min}(e_k), \bar{l}^{\max}(e_k)]$ obtained by triangle inequality from extreme linkages of the last extreme graph $\hat{G}_f(k)$, and map back to obtain a set S_0 of intervals for l_f .

```

 $S_k \leftarrow \{[\bar{l}^{\min}(e_k), \bar{l}^{\max}(e_k)]\}$ 
for  $i = k - 1$  to 0
  [Map the interval of  $l(e_{i+1})$  back to  $l(e_i)$ ]
  if  $e_{i+1}$  and  $e_i$  satisfy the requirement in Lemma 1 (a)
    Obtain  $S_i$  from  $S_{i+1}$  using mapping with the ellipse  $\mathcal{C}$ 
    [ $e_{i+1}$  and  $e_i$  are two diagonals of a quadrilateral]
  else [ $e_{i+1}$  and  $e_i$  satisfy the requirement in Lemma 1 (b)]
    if  $e_{i+1}$  and  $e_i$  connect the same pair of adjacent clusters in the four-cycle
      Obtain  $S_i$  from  $S_{i+1}$  by the law of cosines
      [see Remark 5(a) in Appendix D]
    else
      Obtain  $S_i$  from  $S_{i+1}$  by the law of cosines and mapping with  $\mathcal{C}$ 
      [see Remark 5(b) in Appendix D]
return  $S_0$ 

```

Lemma 2 (QIM for 1-path). For a 1-path tree-decomposable linkage (G, \bar{l}) where G has low Cayley complexity on f , the set S_0 of intervals for l_f generated by the QIM algorithm is exactly the Cayley configuration space over f .

The proof of Lemma 2 is given in Appendix D.

We give two examples to demonstrate how the QIM algorithm works.

Example 1:

To obtain the Cayley configuration space on $f = (v_0, v'_0)$ for G in Figure 11(a):

- **Step 1:** Obtain the interval of $l(v_4, v_2)$ in $\Delta v_2 v_4 v_5$ by triangle inequality;
- **Step 2:** In quadrilateral $v'_0 v_2 v_3 v_4$, obtain the interval of $l(v'_0, v_3)$ from the interval of $l(v_4, v_2)$;
- **Step 3:** Similarly, in quadrilateral $v'_0 v_1 v_3 v_2$, we have $l(v'_0, v_3) \rightarrow l(v_1, v_2)$;
- **Step 4:** In quadrilateral $v_0 v_2 v'_0 v_1$, we have $l(v_1, v_2) \rightarrow l(v_0, v'_0)$.

Example 2:

To obtain the Cayley configuration space on $f = (v_0, v'_0)$ for G in Figure 14:

- **Step 1:** Obtain the interval of $l(u_2, v_3)$ in $\Delta v_4 v_3 u_2$ by triangle inequality;
- **Step 2:** In four-cycle $T'_2 T_3 T'_3 T'_1$, we have $l(u_2, v_3) \rightarrow l(u_1, u'_1)$;
- **Step 3:** In four-cycle $T'_2 T'_1 T_1 T_2$, we have $l(u_1, u'_1) \rightarrow l(v_0, v'_0)$.

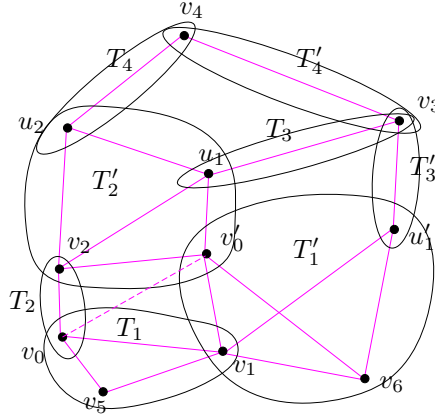


Figure 14: Example 2: QIM on a 1-path graph. See also a demonstration video at <http://www.cise.ufl.edu/~menghan/caymos/qim.avi>.

The worst-case time complexity of the QIM algorithm is exponential in the number of construction steps, since each mapping could possibly double the number of intervals. Nevertheless, when the minimal realization type is fixed, using the QIM algorithm, we can obtain the Cayley configuration space of a 1-path graph in linear time.

Proposition 1 (fixed minimal realization type for 1-path). *For a 1-path, 1-dof, tree-decomposable graph G with low Cayley complexity on f , if the minimal realization type is fixed, for any linkage (G, \bar{l}) , the Cayley configuration space over f contains at most one interval, and can be found in $O(|V|)$ time.*

Proof. When the minimal realization type is fixed, when applying QIM to any linkage with underlying graph G , we are restricted to a monotonic segment of the ellipse \mathcal{C} . We start from a single interval for the last extreme edge of G and map back to f . Since we are always mapping using monotonic segment of \mathcal{C} , the image is at most one interval. Therefore, l_f , as well as each of the distances between base pairs of vertices, takes values in at most one attainable interval (the interval depends on the base pair). So each construction step takes constant time. Since the number of construction steps is $O(|V|)$, the Cayley configuration space can be computed in $O(|V|)$ time. \square

Next, we will look at the general case, where a graph can have more than one path, namely, more than one vertex at the last level L_t (other than the endpoints of the given base non-edge). We say that each such last level vertex corresponds to a *path*.

Lemma 3 (QIM for multi-path). *For a 1-dof tree-decomposable graph G with low Cayley complexity on $f = (v_0, v'_0)$, if the minimal realization type is fixed, we can use the QIM algorithm to correctly find the Cayley configuration space over f for any linkage (G, \bar{l}) , and this Cayley configuration space is a single interval.*

Proof. Consider a linkage (G, \bar{l}) with $k+1$ paths. For any vertex v_i in the last level L_t different from v_0 and v'_0 , there exists a sequence of construction steps from f to v_i , such that v_i depends on all these construction steps. We call this construction sequence *the i^{th} path p_i of G* , which is in fact a 1-path subgraph. By Proposition 1, for each p_i , we can apply the QIM algorithm for 1-path linkages to find its Cayley configuration space over f , which is a single interval I_i . Then we take the intersection $I = \bigcap_{1 \leq i \leq k} I_i$, which is also a single interval.

By induction hypothesis, each path (p_i, \bar{l}) is realizable if and only if l_f is in I_i , so if $l_f \notin I$, the linkage is not realizable. On the other hand, since the minimal realization type is fixed, when $l_f \in I$, all paths are simultaneously realizable (each value of l_f corresponds to a unique realization of the entire linkage). Therefore, I is the Cayley configuration space of (G, \bar{l}) over f . \square

Finally, we can prove the main theorem.

Proof of Theorem 2. By Lemma 3, for any linkage with underlying graph G , the Cayley configuration space over f contains at most a single interval. The QIM algorithm takes $O(|V|)$ time on each path, and there can be at most $O(|V|)$ paths, so the Cayley computational complexity is $O(|V|^2)$. \square

Remark 3. This result shows the advantage of the QIM algorithm over the ELR algorithm we mentioned in Section 3. First, realizing each extreme linkage takes $O(|V|)$ time, therefore realizing all $O(|V|)$ extreme linkages from f takes $O(|V|^2)$ time. Moreover, note that when the reverse realization type is fixed, an interval endpoint can also arise from a change in reverse realization type. This is not an extreme linkage for the given base non-edge, but an extreme linkage for an extreme non-edge. So the ELR algorithm must consider extreme linkages for all these $O(|V|)$ possible base non-edges, and the overall time complexity is $O(|V|^3)$.

Why does the QIM algorithm fails as is, if the minimal realization type is not fixed? Notice that when the minimal realization type is not fixed, we cannot simply take intersection of intervals as in proof of Lemma 3, since realizations requiring different minimal realization types can generate the same l_f . For example, refer to Figure 11 (b). There are two paths, p_0 and p_1 , corresponding to vertices v_5 and v_6 in the last level respectively. For certain \bar{l} , p_1 may require v_1 and v_4 to be on the same side of (v_3, v'_0) such that v_6 can be realized. At the same time, p_0 may require v_1 and v_4 to be on different sides of (v_3, v'_0) such that v_5 can be realized. These two different realization types can generate the same l_f . If we just take intersection of intervals of values for l_f , even the intersection is non-empty, the linkage may still be unrealizable since p_0 and p_1 require conflicting realization types. An alternative strategy would be to follow the construction steps, and perform $O(|V|)$ mappings altogether.

The above discussion leads to the following conjecture:

Conjecture 1. *Even when the minimal realization type is not fixed, the QIM algorithm can be adapted to work for 1-dof tree-decomposable linkages whose underlying graphs have low Cayley complexity. When the minimal realization type is fixed, this adapted algorithm can be used to obtain the Cayley configuration space in $O(|V|)$ time.*

Implementation of the algorithms discussed in this paper for finding Cayley configuration spaces is part of our new CayMos software, whose architecture is described in [23] and web-accessible at <http://www.cise.ufl.edu/~menghan/caymos/>. See also a video demonstrating QIM algorithm at <http://www.cise.ufl.edu/~menghan/caymos/qim.avi>. A different manuscript [24] describes Cayley and Cartesian configuration space analysis and motion analysis of common and well-known mechanisms using CayMos.

5 Finding a path of continuous motion between two realizations

As we will show below, we can easily find a path of continuous motion between two given realizations, given the oriented Cayley configuration spaces of a linkage whose underlying graph has low Cayley complexity.

Theorem 3 (Continuous motion path Theorem). *For a generic linkage (G, \bar{l}) where G has low Cayley complexity on f ,*

- (i) *Given two realizations, there exist at most two paths of continuous motion between them, and the time complexity of finding such a path (provided one exists) is linear in the number of interval endpoints of oriented Cayley configuration spaces that the path contains.*
- (ii) *Given two realizations with the same minimal realization type, there exists a unique path of continuous motion between them, staying within the same minimal realization type, and the time complexity of finding that path is $O(1)$.*

Idea of the proof. The genericity is very important here. We analyze the continuous motion of the linkage in Lemma 4 (continuous motion inside an interval) and Lemma 5 (change of realization type), proving that the realization type can only be changed via extreme linkages at interval endpoints of oriented Cayley configuration spaces, and (i) directly follows. Then we apply Theorem 2 (fixed minimal realization type) to get (ii).

We mentioned in Remark 2 that an extreme linkage realization may be an internal point of an interval in the unoriented Cayley configuration space. We now show that every extreme linkage realization corresponds to an interval endpoint of the oriented Cayley configuration space.

Lemma 4 (continuous motion inside an interval). *(i) Between two points lying in the same interval of an oriented Cayley configuration space, there always exists a unique path of continuous motion staying within that interval.*

(ii) No extreme linkage realization can correspond to an internal point of an interval in any oriented Cayley configuration space.

Lemma 5 (change of realization type). *During continuous motion, a linkage whose underlying graph has low Cayley complexity can only change forward realization type via endpoints of oriented Cayley configuration spaces, and only one entry of the forward realization type is switched by such a change.*

The proofs of Lemma 4 and 5 are given in Appendix E.

Proof of Theorem 3. For (i), the following algorithm finds a path of continuous motion between two realizations in time linear in the number of endpoints along that path:

From the starting realization $G(p_s)$ with forward realization type σ , we take the oriented Cayley configuration space for realization type σ and find the interval I_σ that $G(p_s)$ is in. By Lemma 4 (i), inside I_σ there always exists a path of continuous motion. Take one endpoint $l_f = l_0$ of I_σ . In the corresponding realization $G(p_0)$, exactly one entry, say entry i , of the forward realization type is 0. By Lemma 5, the next immediately reachable oriented Cayley

configuration space is uniquely determined, since its realization type τ should be the same as σ except having the opposite sign in entry i . Since intervals in an oriented Cayley configuration space are all disjoint, there is at most one interval in the oriented Cayley configuration space for realization type τ with l_0 as an endpoint. So we can find at most one interval I_τ immediately reachable. We repeat the process from the other endpoint of I_τ until we reach the interval containing the target realization, or we may go back to the starting interval I_σ , in that case there is no continuous motion path between the two given realizations. Each endpoint encountered leads to at most one next immediately reachable interval, so backtracking is never necessary. Therefore the time complexity is linear in the number of endpoints along the path we found. Since both endpoints of I_σ could potentially lead to the target realization, there are *at most two paths* between two given realizations.

For (ii), by Theorem 2, the two realizations lie in a single interval I_σ in the corresponding oriented Cayley configuration space. By Lemma 4 (i), within a single interval of an oriented Cayley configuration space, there is always a continuous motion path. Therefore, there always exists a unique path maintaining the minimal realization type between the two realizations within I_σ . The time complexity of finding this path is $O(1)$. \square

Figure 3 gives an example running of the algorithm described in the proof above, finding a path of continuous motion from realization (B1) with realization type σ to (B2) with realization type τ . We start from the interval I_σ containing (B1) and take one endpoint of I_σ , which corresponds to extreme linkage realization (A1). Taking the entry of σ which is 0 in (A1), and reversing its sign in σ , we get the next realization type τ . Now we go from (A1) to (A2), which is essentially the same realization but contained in the oriented Cayley configuration space for realization type τ , and the immediately reachable interval I_τ with (A2) as an endpoint realization is uniquely determined. Since I_τ contains the target realization (B2), a continuous path is successfully found.

Remark 4. 1. For Theorem 3 (ii), a second path of continuous motion could exist, if we remove the requirement that the path should stay within the same minimal realization type. In that path, the linkage leaves I_σ from the endpoint closer to the starting realization than the target realization, takes various minimal realization types along the path, and reaches the target realization via the other endpoint of I_σ . By Theorem 3 (i), the time complexity of finding this path is linear in the number of interval endpoints contained in it.

2. Not much improvement of the length of the paths is possible beyond Theorem 3 (i), if the two realizations have either the same forward realization type or the same reverse realization type. When the two realizations have the same forward realization type, the two realizations may belong to different intervals of the corresponding oriented Cayley configuration space. When the two realizations have the same reverse realization type, the two realizations may belong to different oriented Cayley configuration spaces. In both cases, it is not guaranteed that a path of continuous motion exists, and even if such a path exists, the number of interval endpoints contained in it is hard to determine.

Corollary 1 (continuous motion paths between Cayley configurations). *To obtain a continuous path between two Cayley configurations where their forward realization types are unspecified, we run the algorithm given by Theorem 3 (i) for each candidate forward realization type of the starting Cayley configuration and each candidate forward realization type of the target Cayley configuration.*

Note. For each pair of starting and target realizations there are at most two paths, but the number of such pairs could be exponential in the size of the linkage.

Implementation of the algorithms discussed above for finding a continuous motion paths is part of our new CayMos software, whose architecture is described in [23] and web-accessible at <http://www.cise.ufl.edu/~menghan/caymos/>. See also a demonstration video at <http://www.cise.ufl.edu/~menghan/caymos/motion.avi>, and the screen-shot in Figure 15. A

different manuscript [24] describes Cayley and Cartesian configuration space analysis and motion analysis of common and well-known mechanisms using CayMos.

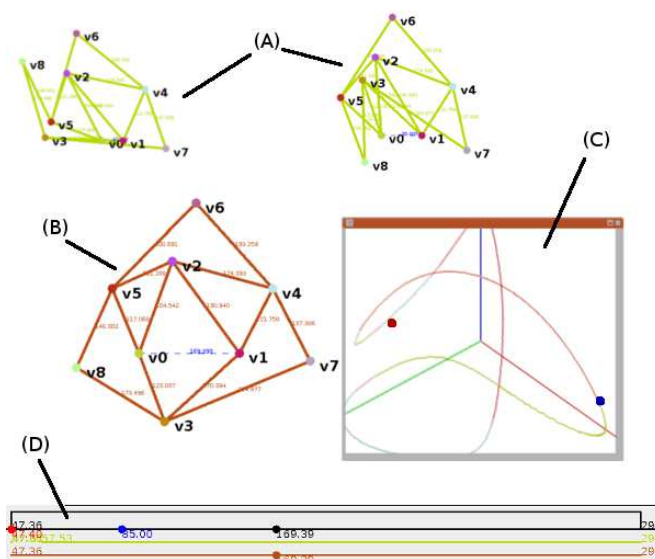


Figure 15: Finding a continuous motion path using our new CayMos software [23] between two realizations. (A) The start and end realizations. (B) The current realization, moving as the user traces the continuous motion path. (C) The 3D projection of the current connected component in the motion space. (D) The intervals of the oriented Cayley configuration spaces encountered along the path.

5.1 Canonical bijective representation of the realization space as curves in an ambient space of minimum/minimal dimension

In this section, we deal with the problem of bijectively representing the realization space of 1-dof tree-decomposable linkages with low Cayley complexity, which yields a meaningful visualization of the realization space and continuous motion. In [24], we have given a bijective representation of the realization spaces using *complete Cayley vectors*. In this paper, we prove Theorem 4 which greatly reduce the dimension of complete Cayley vectors. Specifically, for linkages with 1-path underlying graphs, we achieve the minimum possible dimension of the complete Cayley vector, which is 2.

Important Note: the bijective representation of minimal dimension requires the assumption that the clusters are globally rigid, and clusters sharing only two vertices with the rest of the graph be reduced into edges.

Given a 1-dof tree-decomposable linkage (G, \bar{l}) , where G has low Cayley complexity as well as a 1-path construction from base non-edge $f = (v_0, v'_0)$, with v_n as the last constructed vertex, we define a minimum *complete Cayley vector* F as follows. (1) If G has only one construction step, $F = \langle f \rangle$. (2) If G has two or more construction steps, $F = \langle f, f_1 \rangle$, where $f_1 = (v_0, v_n)$ if (v_0, v_n) is a non-edge of G , otherwise $f = (v'_0, v_n)$.

The definition of a minimal *complete Cayley vector* for a general 1-dof tree-decomposable linkage is given in Appendix F.

The minimal *complete Cayley distance vector* of a realization $G(p)$ is the vector of distances for the non-edges in the complete Cayley vector.

Lemma 6 (1-path global rigidity). *For a 1-path, 1-dof tree-decomposable graph (G, \bar{l}) with low Cayley complexity, adding the non-edges in the minimum complete Cayley vector as edges makes G globally rigid; i.e., any 2D linkage with G as the underlying graph has at most one realization.*

The proof is given in Appendix F.

Lemma 7 (multi-path global rigidity). *For a 1-dof tree-decomposable graph (G, \bar{l}) with low Cayley complexity, adding the non-edges in the minimal complete Cayley vector as edges makes G globally rigid; i.e., any 2D linkage with G as the underlying graph has at most one realization.*

The proof is given in Appendix F.

Proposition 2 (minimality of representation). *(1) For a 1-path, 1-dof tree-decomposable graph with low Cayley complexity, the minimum complete Cayley vector F contains the minimum number of edges that make G globally rigid.*

(2) For a 1-dof tree-decomposable graph with low Cayley complexity, either the minimal complete Cayley vector F is a minimal set of edges that makes G globally rigid, or $F \setminus \{f\}$ is a minimal set of edges that makes G globally rigid, where f is the given base non-edge of the graph.

The proof is straightforward.

Theorem 4 (bijectivity of representation). *(1) For a generic 1-path, 1-dof tree-decomposable linkage with low Cayley complexity, there exists a bijective correspondence between the set of Cartesian realizations and points on a curve in \mathbb{R}^2 , whose points are the minimum complete Cayley distance vectors.*

(2) For a generic 1-dof tree-decomposable linkage with low Cayley complexity, there exists a bijective correspondence between the set of Cartesian realizations and points on a curve in n -dimension, whose points are the minimal complete Cayley distance vectors, where n is the number of last level vertices of the underlying graph.

Proof. Given a Cartesian realization, the minimum or minimal complete Cayley distance vector is uniquely determined. Conversely, given a realizable complete Cayley distance vector, using Lemma 6 and 7, we obtain a unique Cartesian realization since the linkage is generic. Therefore we have a bijective correspondence between the set of Cartesian realizations and the set of minimum or minimal complete Cayley distance vectors. \square

Given a generic 1-dof tree-decomposable linkage with low Cayley complexity, we can visualize the realization space using the *canonical Cayley curve* [24], which is formed by the set of complete Cayley distance vectors representing each realization in the realization space. The complete Cayley distance vector also enables us to define a canonical distance between two connected components, and distance separating two realizations without continuous motion path between them [24].

Implementation of the algorithms discussed above is part of our new CayMos software, whose architecture is described in [23] and web-accessible at <http://www.cise.ufl.edu/~menghan/caymos/>. See also a demonstration video at <http://www.cise.ufl.edu/~menghan/caymos/motion.avi>, and the screen-shot in Figure 15. A different manuscript [24] describes Cayley and Cartesian configuration space analysis and motion analysis of common and well-known mechanisms using CayMos.

6 Conclusion

In Part I of this paper, we investigated the structure of Cayley configuration spaces for 1-dof tree-decomposable linkages, introduced the complexity measures associated with the underlying graphs, and formally gave algorithms to obtain such Cayley configuration spaces. For linkages whose underlying graphs have low Cayley complexity, we gave sufficient and necessary condition for small Cayley size and low Cayley computational complexity. We also gave an efficient algorithm to find a path of continuous motion for such linkages.

Implementation of the algorithms developed in Part I and Part II and further functionalities is part of our new CayMos software, described in [23] and web-accessible at <http://www.cise.ufl.edu/~menghan/caymos/>. A different manuscript [24] includes Cayley and Cartesian configuration space analysis and motion analysis of common and well-known mechanisms.

References

- [1] Ciprian Borcea and Ileana Streinu. The number of embeddings of minimally rigid graphs. *Discrete and Computational Geometry*, 31:287–303, 2004. 10.1007/s00454-003-2902-0.
- [2] Arthur Cayley. A theorem in the geometry of position. *Cambridge Mathematical Journal*, 2(1841):267–271, 1841.
- [3] R. Connelly, E.D. Demaine, and G. Rote. Straightening polygonal arcs and convexifying polygonal cycles. In *Foundations of Computer Science, 2000. Proceedings. 41st Annual Symposium on*, pages 432–442. IEEE, 2000.
- [4] Ioannis Fudos and Christoph M. Hoffmann. Correctness proof of a geometric constraint solver. *International Journal of Computational Geometry and Applications*, 6(4):405–420, 1996.
- [5] Ioannis Fudos and Christoph M. Hoffmann. A graph-constructive approach to solving systems of geometric constraints. *ACM Trans. Graph.*, 16(2):179–216, April 1997.
- [6] H. Gao and M. Sitharam. Combinatorial classification of 2d underconstrained systems. In *Proceedings of the Seventh Asian Symposium on Computer Mathematics (ASCM 2005)*, pages 118–127, 2005.
- [7] Heping Gao and Meera Sitharam. Characterizing 1-dof Henneberg-I graphs with efficient configuration spaces. In *Proceedings of the 2009 ACM symposium on Applied Computing, SAC '09*, pages 1122–1126, New York, NY, USA, 2009. ACM.
- [8] Jack Graver, Brigitte Servatius, and Herman Servatius. *Combinatorial rigidity.*, volume 2 of *Graduate Studies in Mathematics*. American Mathematical Society, Providence, RI, 1993.
- [9] Marta R Hidalgo and Robert Joan-Arinyo. The reachability problem in constructive geometric constraint solving based dynamic geometry. *Journal of Automated Reasoning*, pages 1–24, 2011.
- [10] Bill Jackson and JC Owen. Radically solvable graphs. *arXiv preprint arXiv:1207.1580*, 2012.
- [11] R. Joan-Arinyo, A. Soto-Riera, S. Vila-Marta, and J. Vilaplana-Pastó. Transforming an under-constrained geometric constraint problem into a well-constrained one. In *Proceedings of the eighth ACM symposium on Solid modeling and applications*, SM '03, pages 33–44, New York, NY, USA, 2003. ACM.

- [12] A.B. Kempe. On a general method of describing plane curves of the n th degree by linkwork. *Proceedings of the London Mathematical Society*, s1-7(1):213–216, 1875.
- [13] A.B. Kempe. *How to draw a straight line: a lecture on linkages*. Macmillan and co., 1877.
- [14] G. Laman. On graphs and rigidity of plane skeletal structures. *Journal of Engineering Mathematics*, 4:331–340, 1970. 10.1007/BF01534980.
- [15] Rüdiger Loos. Computing in algebraic extensions. In *Computer algebra*, pages 173–187. Springer, 1983.
- [16] J.C. Owen and S.C. Power. The non-solvability by radicals of generic 3-connected planar laman graphs. *Transactions of the American Mathematical Society*, 359(5):2269–2304, 2007.
- [17] G. Rote, F. Santos, and I. Streinu. Expansive motions and the polytope of pointed pseudo-triangulations. In *Discrete and Computational Geometry-The Goodman-Pollack Festschrift, Algorithms and Combinatorics*, 2003.
- [18] E. Sacks and L. Joskowicz. *The configuration space method for kinematic design of mechanisms*. The MIT Press, 2010.
- [19] J.B. Saxe. Embeddability of weighted graphs in k -space is strongly np-hard. In *Proceedings of 17th Allerton Conference in Communications, Control and Computing*, pages 480–489, 1979.
- [20] M. Sitharam. Combinatorial approaches to geometric constraint solving: Problems, progress, and directions. In: *DIMACS: Series in Discrete Mathematics and Theoretical Computer Science*, 67:117, 2005.
- [21] M. Sitharam and H. Gao. Characterizing graphs with convex and connected configuration spaces. *Arxiv preprint arXiv:0809.3935*, 2008.
- [22] Meera Sitharam, Adam Arbree, Yong Zhou, and Naganandhini Kohareswaran. Solution space navigation for geometric constraint systems. *ACM Trans. Graph.*, 25(2):194–213, April 2006.
- [23] Meera Sitharam and Menghan Wang. Cayley configuration space analysis by CayMos: software architecture and functionalities. Software available at: <http://www.cise.ufl.edu/~menghan/caymos/>, in preparation, 2013.
- [24] Meera Sitharam and Menghan Wang. How the beast really moves: Cayley analysis of mechanism realization spaces using caymos. *Computer-Aided Design*, 46(0):205 – 210, 2014. 2013 SIAM Conference on Geometric and Physical Modeling.
- [25] Ileana Streinu. A combinatorial approach to planar non-colliding robot arm motion planning. *Proc. 41st IEEE Annual Symposium on Foundations of Computer Science (FOCS)*, pages 443–453, 2000.
- [26] Ileana Streinu. Pseudo-triangulations, rigidity and motion planning. *Discrete and Computational Geometry*, 34(4):587–635, November 2005.
- [27] H.A. van der Meiden and W.F. Bronsvoort. A constructive approach to calculate parameter ranges for systems of geometric constraints. *Computer-Aided Design*, 38(4):275–283, 2006.
- [28] Zhiyuan Ying and S. Sitharama Iyengar. Robot reachability problem: A nonlinear optimization approach. *Journal of Intelligent and Robotic Systems*, 12:87–100, 1995. 10.1007/BF01258308.

- [29] G.F. Zhang and X.S. Gao. Well-constrained completion and decomposition for under-constrained geometric constraint problems. *International Journal of Computational Geometry and Applications*, 16(5-6):461–478, 2006.

A Proof of Theorem 1 (structure of Cayley configuration space)

In the following, we denote the Cayley configuration space of a 1-dof tree-decomposable linkage (G, \bar{l}) over f by $\Phi_f(G, \bar{l})$, and the oriented Cayley configuration space with forward realization type σ by $\Phi_f(G, \bar{l}, \sigma)$.

Proof. We first prove for a fixed forward realization type σ , that the theorem holds for the oriented Cayley configuration space, by induction on the number of construction steps from f .

In the base case, G has only one construction step $v_1 \triangleleft (v_0 \in T_1, v'_0 \in T_2)$. The distances $\bar{l}(v_1, v_0)$ and $\bar{l}(v_1, v'_0)$ are fixed by clusters T_1 and T_2 respectively, and by triangle inequality, $\Phi_f(G, \bar{l}, \sigma)$ is a single closed interval $[|\bar{l}(v_1, v_0) - \bar{l}(v_1, v'_0)|, \bar{l}(v_1, v_0) + \bar{l}(v_1, v'_0)]$. Clearly, (1) and (2) hold. For (3), without loss of generality, let $p(v_0)$ be the origin, $p(v'_0)$ lie on the x -axis, and $p(v_1) = (x_1, y_1)$ has positive y -coordinate. Let $R_1 = \bar{l}(v_1, v_0)$, $R_2 = \bar{l}(v_1, v'_0)$ and $R_3 = l(v_0, v'_0) = l_f$. In $\triangle v_0 v'_0 v_1$, we have

$$x_1 = \frac{R_1^2 + R_3^2 - R_2^2}{2R_3} \cdot \sigma_1$$

$$y_1 = \frac{\sqrt{(R_1 + R_2 + R_3)(R_1 + R_2 - R_3)(R_1 - R_2 + R_3)(-R_1 + R_2 + R_3)}}{2R_3}$$

where σ_1 is the entry corresponding to the first construction step in the forward realization type σ .

Since the linkage is generic, R_3 , namely l_f , cannot be 0, so both x_1 and y_1 are continuous functions of l_f . Moreover, since internal realizations of both T_1 and T_2 are uniquely specified, the coordinates of all other vertices in T_1 and T_2 are continuous functions of coordinates of v_1 , v_0 and v'_0 , thus continuous functions of l_f .

As induction hypothesis, assume that the theorem holds for linkages whose underlying graph $G_f(k-1)$ has $k-1$ construction steps. Consider a graph $G_f(k)$ with k construction steps, obtained by adding one more construction step $v_k \triangleleft (u_k \in T_1, w_k \in T_2)$ to $G_f(k-1)$. For any linkage $(G_f(k), \bar{l})$, according to Statement (3) of the induction hypothesis, $l(u_k, w_k)$ is a continuous function of l_f , say $l(u_k, w_k) = g(l_f)$. By triangle inequality, $l(u_k, w_k)$ is restricted to the interval $[\min, \max]$ where $\min = |\bar{l}(u_k, v_k) - \bar{l}(w_k, v_k)|$ and $\max = \bar{l}(u_k, v_k) + \bar{l}(w_k, v_k)$. This restriction may create new candidate interval endpoints in $\Phi_f(G_f(k), \bar{l}, \sigma)$, namely $g^{-1}(\min)$ and $g^{-1}(\max)$, as shown in Figure 16. A candidate endpoint is actually a new interval endpoint, only if its corresponding extreme linkage realization $p(\hat{G}_f(k), \bar{l}^{\min}, \sigma)$ (resp. $p(\hat{G}_f(k), \bar{l}^{\max}, \sigma)$) does exist. So (1) and (2) also hold for $(G_f(k), \bar{l})$.

To prove (3), take any vertex v in $G_f(k)$. By induction hypothesis, if $v \notin (T_1 \cup T_2)$, $p(v)$ is a continuous function of l_f . For $v \in (T_1 \cup T_2)$, we first consider $p(v_k)$. For convenience, first rotate and translate the coordinate system so that $p(u_k)$ is at the origin, $p(w_k)$ is on the x -axis, and $p(v_k) = (x_k, y_k)$ have positive y -coordinate. Let $R_1 = \bar{l}(v_k, u_k)$, $R_2 = \bar{l}(v_k, w_k)$ and $R_3 = l(u_k, w_k)$. In $\triangle u_k w_k v_k$, we have

$$x_k = \frac{R_1^2 + R_3^2 - R_2^2}{2R_3} \cdot \sigma_k$$

$$y_k = \frac{\sqrt{(R_1 + R_2 + R_3)(R_1 + R_2 - R_3)(R_1 - R_2 + R_3)(-R_1 + R_2 + R_3)}}{2R_3}$$

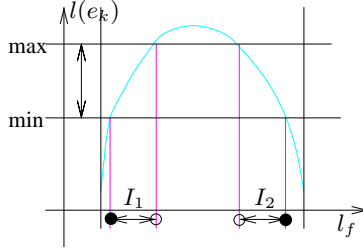


Figure 16: For Theorem 1. New constraint on $l(u_k, w_k)$ creating interval endpoints in $\Phi_f(G_f(k), \bar{l})$. \bullet : $g^{-1}(\min)$; \circ : $g^{-1}(\max)$.

where σ_k is the entry corresponding to the k^{th} construction step in the forward realization type σ .

Since the linkage is generic, $R_3 > 0$. So both x_k and y_k are continuous functions of l_f . Moreover, since internal realizations for both T_1 and T_2 are specified, the coordinates of any other $v \in (T_1 \cup T_2)$ are continuous functions of $p(u_k)$, $p(v_k)$ and $p(w_k)$, thus continuous functions of l_f . Consequently, for any non-edge (u, w) , $l(u, w)$ is also a continuous function of l_f . Note that this continuity is not affected even if we transform back to the original coordinate system.

For the complete Cayley configuration space, (1) and (2) still hold since $\Phi_f(G, \bar{l})$ is just the union of oriented Cayley configuration spaces over all possible forward realization types. \square

B Finding Cayley configuration spaces by realizing all extreme linkages (ELR)

Given a linkage (G, \bar{l}) and a forward realization type σ , in the ELR algorithm, we use a set \mathcal{I}_σ to store candidate intervals of the oriented Cayley configuration space, which is initially the entire \mathbb{R}^1 . For each realization step i , we update \mathcal{I}_σ by considering restrictions on l_f from all extreme linkage realizations of $\hat{G}_f(i)$ with forward realization type σ . After we have done this for every realization step, \mathcal{I}_σ is the oriented Cayley configuration space.

Algorithm (ELR):

```

 $\mathcal{I}_\sigma \leftarrow (-\infty, +\infty)$ 
for  $i = 1$  to  $k$  do   [ $k$  is the number of  $G$ 's construction steps]
   $S \leftarrow \emptyset$    [set of candidate interval endpoints]
  for every extreme linkage realization  $p$  of  $\hat{G}_f(i)$  with forward realization type  $\sigma$ 
    if  $(G \cup f, \bar{l} \cup l_f)$  is realizable
      add  $l_f$  value of  $p$  to  $S$ 
  for each candidate endpoint  $l_0$  in  $S$ 
    UPDATE( $\mathcal{I}_\sigma, l_0$ )   [see following discussion]
return  $\mathcal{I}_\sigma$ 

```

When updating \mathcal{I}_σ , we need to notice that not every candidate Cayley configuration l_0 in S actually creates new restriction on \mathcal{I}_σ . Recall from the proof of Theorem 1 that a realization step $v_i \triangleleft (u_i, w_i)$ restricts $l(u_i, w_i) = g(l_f)$ in $[\min, \max]$. As shown in Figure 17, there are three possible cases for a candidate configuration l_0 : (a) both the left and the right neighborhood of l_0 fall into \mathcal{I}_σ ; (b) the left neighborhood of l_0 falls into \mathcal{I}_σ but the right does not, and symmetrically, the right neighborhood falls into \mathcal{I}_σ but the left does not; (c) neither the left nor the right neighborhood of l_0 falls into \mathcal{I}_σ , meaning that l_f itself is the only realization in the neighborhood. In (b), l_0 creates a new endpoint in \mathcal{I}_σ . In (c), l_0 creates an isolated point in \mathcal{I}_σ . In (a), l_0 does not create any interval endpoint in \mathcal{I}_σ .

So in the UPDATE procedure, for each candidate Cayley configuration l_0 , we check if there

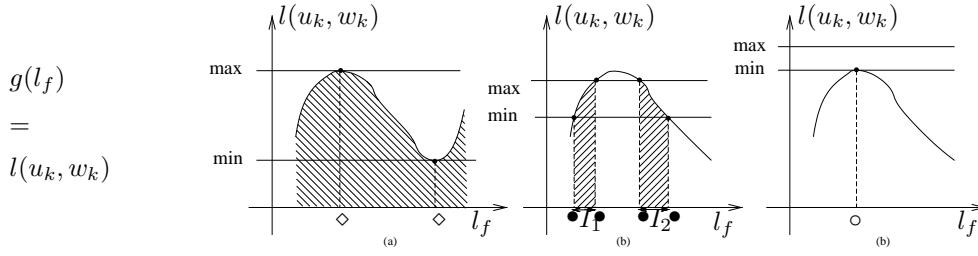


Figure 17: $\min = |\bar{l}(v_k, u_k) - \bar{l}(v_k, w_k)|$, $\max = \bar{l}(v_k, u_k) + \bar{l}(v_k, w_k)$. (a) candidate l_f values \diamond that are internal points of some interval in \mathcal{I}_σ , not endpoints; (b) candidate l_f values \bullet that are new interval endpoints in \mathcal{I}_σ , creating intervals I_1 and I_2 ; (c) candidate l_f value \circ that creates an isolated point in \mathcal{I}_σ .

is any realization, with l_f value between l_0 and the immediately preceding (resp. immediately succeeding) candidate interval endpoint in \mathcal{I}_σ .

Algorithm: UPDATE($\mathcal{I}_\sigma, l_f^{\min}, l_f^{\max}$)
 $prev \leftarrow \max\{l \in \mathcal{I}_\sigma \mid l < l_0\}$, $next \leftarrow \min\{l \in \mathcal{I}_\sigma \mid l > l_0\}$
 $p \leftarrow (prev + l_0)/2$, $n \leftarrow (next + l_0)/2$
 $P \leftarrow true$ if p has corresponding realization, *false* otherwise
 $N \leftarrow true$ if n has corresponding realization, *false* otherwise
if exactly one of P and N is *true*
 add l_0 as an endpoint in \mathcal{I}_σ
elseif both P and N are *false*
 add l_0 as an (isolated) endpoint to \mathcal{I}_σ

To obtain the complete Cayley configuration space, we just take $\Phi_f(G, \bar{l}) = \bigcup_{\sigma} \mathcal{I}_\sigma$.

C Exponential blow-up of Cayley size and Cayley complexity when the minimal realization type is not specified

We provide in this section an example, that the Cayley size of a graph with low Cayley complexity can be exponential in $|V|$, even when a forward realization type is specified. One can use a symmetric example to show that if we just fix the reverse realization type, there can be exponentially many non-empty oriented Cayley configuration spaces.

Observation 3. *The Cayley size of a graph with low Cayley complexity can be exponential in the number of construction steps if we only fix the forward realization type.*

Proof. We give an example of a 1-dof tree-decomposable linkage (G, \bar{l}) with a fixed forward realization type σ and low Cayley complexity, which has exponential Cayley size. See Figure 18. The base non-edge is $f = f_1 = (v_1, v_3)$. For convenience we slightly abuse our notation to let the construction step number start from 0, so the 0th and 1st construction steps are $v_4 \triangleleft (v_1, v_3)$ and $v_2 \triangleleft (v_1, v_3)$ respectively. They form the outermost quadrilateral $Q_1 = v_4 v_3 v_2 v_1$.

For every $k > 1$, the k^{th} construction step is $v_{k+3} \triangleleft (v_{k+2}, v_k)$, which appends one vertex and two edges to the graph, and forms a nested quadrilateral $Q_k = v_{k+3} v_{k+2} v_{k+1} v_k$. We denote the four edges of Q_k as $(v_{k+3}, v_{k+2}) = s_{k,1}$, $(v_{k+2}, v_{k+1}) = s_{k,2}$, $(v_{k+1}, v_k) = s_{k,3}$ and $(v_k, v_{k+3}) = s_{k,4}$, and two diagonals $(v_{k+3}, v_{k+1}) = f_{k+1}$, $(v_{k+2}, v_k) = f_k$. Notice that Q_k shares two edges with Q_{k-1} : $s_{k,2} = s_{k-1,1}$, $s_{k,3} = s_{k-1,2}$. The forward realization type σ is assigned such that v_{k+3} and v_{k+1} lies on different side of f_k .

Clearly, G is 1-path with low Cayley complexity. So we use the QIM algorithm introduced in Section 4.1.1 to compute $\Phi_f(G, \bar{l})$. We start from the last extreme edge, and repetitively

map $l(f_k)$ to get intervals for $l(f_{k-1})$, until we obtain the intervals for $l(f_1)$.

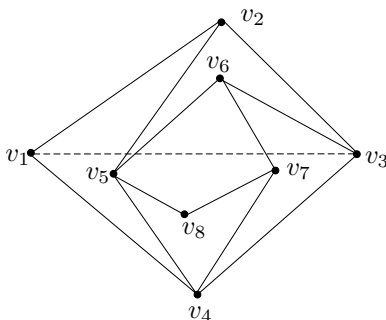


Figure 18: A 1-dof tree-decomposable graph that can have exponential Cayley size for base non-edge $f_1 = (v_1, v_3)$. The graph is a series of nested quadrilaterals and each cluster is an edge.

Example C.1. We choose \bar{l} such that for Q_1 , $\bar{l}(s_{1,1}) = \bar{l}(v_4, v_3) = 8$, $\bar{l}(s_{1,2}) = \bar{l}(v_3, v_2) = 8.1$, $\bar{l}(s_{1,3}) = \bar{l}(v_2, v_1) = 7.9$, $\bar{l}(s_{1,4}) = \bar{l}(v_4, v_1) = 1$. The ellipse \mathcal{C} relating the two diagonals of Q_1 is shown in Figure 19. Only the upper half of the curve (shown in solid line) corresponds to realizations with forward realization type σ .

For each $k > 1$, we assign $\bar{l}(s_{k,1})$ and $\bar{l}(s_{k,4})$ by the following: (1) Observe the ellipse \mathcal{C} of Q_{k-1} , as shown in Figure 19. Denote the leftmost point on \mathcal{C} by $p_{\min}(f_{k-1})$, the rightmost point by $p_{\max}(f_{k-1})$, the topmost point by $p_{\max}(f_k)$. Let l_2 be the length of f_k at $p_{\max}(f_k)$, and l_1 be the larger one of the lengths of f_k at $p_{\min}(f_{k-1})$ and $p_{\max}(f_{k-1})$. The interval $[l_1, l_2]$ is attainable by $l(f_k)$ in $G_f(k-1)$. (2) Assign $\bar{l}(s_{k,1})$ and $\bar{l}(s_{k,4})$ such that $\bar{l}(s_{k,1}) - \bar{l}(s_{k,4}) = \bar{l}^{\min}(f_k) = (1 + \epsilon)l_1$, $\bar{l}(s_{k,1}) + \bar{l}(s_{k,4}) = \bar{l}^{\max}(f_k) = (1 - \epsilon)l_2$, where ϵ is a positive value small enough so that $\bar{l}(s_{k,1})$ and $\bar{l}(s_{k,4})$ have positive solutions. In this way, $l(f_k)$ is restricted to an interval $[\bar{l}^{\min}(f_k), \bar{l}^{\max}(f_k)]$ slightly tighter than $[l_1, l_2]$.

For example, we want to assign \bar{l} for the 2^{nd} realization step $v_5 \triangleleft (v_4, v_3)$. As shown in Figure 19, in Q_1 , $l_2 = 7.9 + 1 = 8.9$. For $p_{\min}(f_{k-1})$, $l(f_1) = 8 - 1 = 7$, the corresponding $l(f_2) \approx 8.36$. For $p_{\max}(f_{k-1})$, $l(f_1) = 8 + 1 = 9$, the corresponding $l(f_2) \approx 7.42$. Therefore $l_1 = \max[8.36, 7.42] = 8.36$. So let $\bar{l}^{\min}(f_2) = \bar{l}(v_5, v_4) - \bar{l}(v_5, v_3) = (1 + 10^{-5})l_1 \approx 8.364$, $\bar{l}^{\max}(f_2) = \bar{l}(v_5, v_4) + \bar{l}(v_5, v_3) = (1 - 10^{-5})l_2 \approx 8.900$. We assign $\bar{l}(v_5, v_4) \approx 8.632$, $\bar{l}(v_5, v_3) \approx 0.268$. The two new extreme linkages $(\hat{G}_f(2), \bar{l}^{\min})$ and $(\hat{G}_f(2), \bar{l}^{\max})$ each has two realizations, and each of these realizations creates a new endpoint in $\Phi_f(G, \bar{l})$: $(\hat{G}_f(2), \bar{l}^{\max})$ corresponds to realizations in Figure 19 (b) and (d), $(\hat{G}_f(2), \bar{l}^{\min})$ corresponds to realizations in Figure 19 (a) and (c) (point b, d, a and c in the left graph respectively). Since $l_b(f_1) \approx 7.00$, $l_d(f_1) \approx 8.52$, $l_a(f_1) \approx 7.49$, $l_c(f_1) \approx 7.51$, $\Phi_f(G, \bar{l})$ contains two intervals $I_1 = [7.00, 7.49]$ and $I_2 = [7.51, 8.52]$, corresponding to two different reverse realization types.

Table 1 shows \bar{l} for the subsequent construction steps, computed by the procedure described above. Figure 20 shows $\Phi_f(G_f(6), \bar{l})$. The single interval of $l(v_5, v_3)$ maps to 2 intervals for $l(v_2, v_4)$: $I_1 = [8.36, 8.48]$, $I_2 = [8.49, 8.74]$, and 4 intervals for the base non-edge $l(v_1, v_3)$: $I_{11} = [7.000, 7.008]$, $I_{21} = [7.010, 7.121]$, $I_{22} = [8.039, 8.391]$, $I_{12} = [8.403, 8.524]$.

In general, the k^{th} realization step ($k > 1$) produces one interval for $l(f_k)$ which maps to 2 intervals for $l(f_{k-1})$, 4 intervals for $l(f_{k-2})$, and finally 2^{k-1} intervals for $f_1 = (v_1, v_3)$. Notice that there is no overlapping since the curve is monotonic in each interval. \square

D Details of the QIM Algorithm

Remark 5. (a) Refer to (u_2, u'_2) and (u_1, u'_1) in Figure 12 (a). Consider the two triangles $\triangle v_3 u_1 u'_1$ and $\triangle v_3 u_2 u'_2$. Since T_5 and T_6 are fixed clusters, the lengths of triangle edges (v_3, u_1) ,

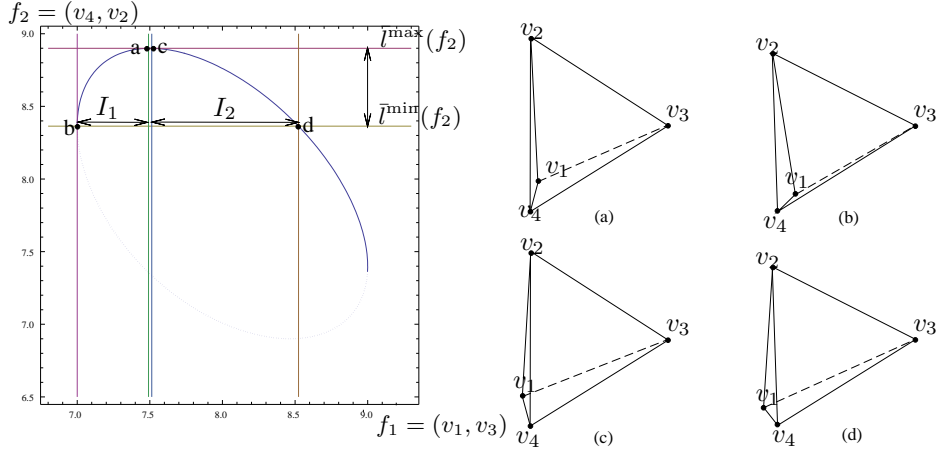


Figure 19: Example C.1. Ellipse \mathcal{C} for quadrilateral $Q_1 = v_4v_3v_2v_1$. Length of extreme edge (v_2, v_4) is restricted by the 2^{nd} realization step, and of $l(v_1, v_3)$ has 2 intervals.

k	$l(s_{k,1})$	$l(s_{k,2})$	$l(s_{k,3})$	$l(s_{k,4})$	number of intervals for $l(v_1, v_3)$ after step k
2	8.632	8	8.1	0.268	2
3	8.306	8.632	8	0.062	4
4	8.044	8.306	8.632	0.017	8
5	8.645	8.044	8.306	0.004	16
6	8.310	8.645	8.044	0.001	32
7	8.045	8.310	8.645	0.0003	64
8	8.645	8.045	8.310	0.00006	128
9	8.310	8.645	8.045	0.00001	256
10	8.045	8.310	8.645	0.000004	512

Table 1: Example C.1. Edge lengths of quadrilateral Q_k for construction step 2 to 10.

(v_3, u'_1) , (v_3, u_2) and (v_3, u'_2) are fixed. Moreover, if we know one of the two angles, $\angle u_1v_3u'_1$ and $\angle u_2v_3u'_2$, we can easily obtain the other. So from a value of $l(u_1, u'_1)$, by the law of cosines, we can obtain $\angle u_1v_3u'_1$ and thus $\angle u_2v_3u'_2$, from which we can get a unique corresponding value of $l(u_2, u'_2)$. Symmetrically, each value of $l(u_2, u'_2)$ corresponds to a unique value of $l(u_1, u'_1)$. (b) Refer to (u_2, u'_2) and (u_1, u'_1) in Figure 12 (b). By (i), there is a one-to-one correspondence between $l(v_3, u'_0)$ and $l(u_2, u'_2)$ with constant time cost. Notice that (v_3, u'_0) and (u_1, u'_1) are the two diagonals of quadrilateral $v_3u_1u'_0u_1$. Therefore we can map to $l(u_1, u'_1)$.

Proof of Lemma 2 (QIM for 1-path). We prove by induction on the number of construction steps of G .

In the base case, there is only one construction step, and the Observation is vacuously true.

As the induction hypothesis, we assume that the algorithm correctly generates the Cayley configuration space for linkages with less than k construction steps. For a graph G with k construction steps, by the Recursive Structure Lemma, there are only two construction steps directly based on $f = (u_0, u'_0)$, and $G' = G \setminus \{u_0, u'_0\}$ (or $G' = G \setminus \{u_0\}$) is a 1-path, 1-dof, tree-decomposable graph with low Cayley complexity on (u_1, u'_1) , and less than k construction steps.

By induction hypothesis, (G', \bar{l}) is realizable if and only if $l(u_1, u'_1)$ is in the set S_1 of intervals generated by applying QIM on (G', \bar{l}) . For QIM on (G, \bar{l}) , we do an additional mapping to get S_0 from S_1 . When l_f belongs to an interval of S_0 , the first four-cycle $v_0u'_1v'_0u_1$ is clearly

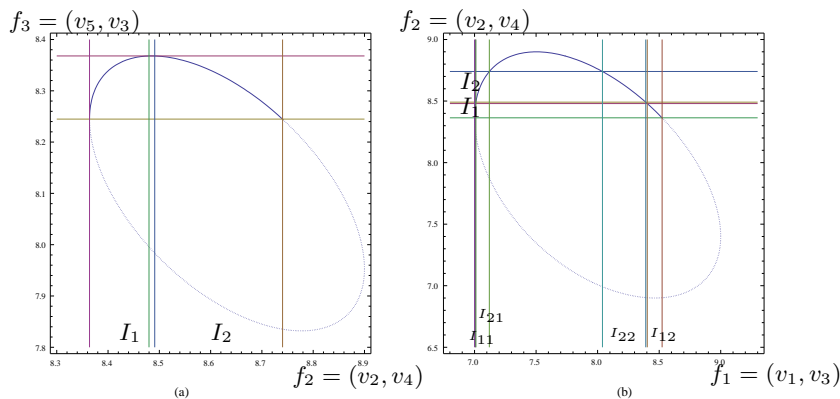


Figure 20: Example C.1. Ellipse \mathcal{C} for quadrilaterals (a) $Q_2 = v_5v_4v_3v_2$ and (b) $Q_1 = v_4v_3v_2v_1$ after v_6 is realized. The Cayley configuration space over (v_1, v_3) is divided into 4 intervals I_{11} , I_{21} , I_{22} , I_{12} .

realizable; moreover, $l(u_1, u'_1)$ is in S_1 since S_0 is generated by mapping from S_1 , so (G', \bar{l}) is also realizable. Thus for all l_f values in S_0 , (G, \bar{l}) is realizable. On the other hand, when l_f is not in any interval of S_0 , either the first four-cycle is not realizable, or (G', \bar{l}) is not realizable, so all realizable l_f values are contained in S_0 . Therefore S_0 is the Cayley configuration space of (G, \bar{l}) over f . \square

E Proofs for the Continuous motion path Theorem

Proof of Lemma 4 (continuous motion inside an interval). (i) Let $l_f = l_1$ and $l_f = l_2$ be in the same interval I_σ in oriented Cayley configuration space $\Phi_f(G, \bar{l}, \sigma)$, and the corresponding realizations be $G(p_1)$ and $G(p_2)$ respectively. By definition of oriented Cayley configuration space, there exists a ruler and compass realization with realization type σ for every Cayley configuration in I_σ between l_1 and l_2 . One can easily verify that this series of realizations gives a path of continuous motion between $G(p_1)$ and $G(p_2)$.

(ii) Assume some extreme graph $\hat{G}_f(k)$ has a corresponding extreme linkage realization $G(p)$, with f 's length $l_f = l_0$ being an internal point of an interval I_σ in oriented Cayley configuration space $\Phi_f(G, \bar{l}, \sigma)$. Since the length l_e^* of the extreme edge e in $G(p)$ is the maximum (resp. minimum) possible value for e 's length $l(e)$, it follows that for all small enough ϵ , the oriented Cayley configurations $l_f = l_0 - \epsilon$ and $l_f = l_0 + \epsilon$ in I_σ both correspond to realizations with $l(e) < l_e^*$ (resp. $l(e) > l_e^*$).

By the proof of Theorem 2 (fixed minimal realization type), $l(e)$ would be a monotonic function of l_f if the minimal realization type is unchanged. Since $l(e)$ increases before l_f reaches l_0 and decreases after l_f reaches l_0 , the minimal realization type must change at l_0 . Since the forward realization type is unchanged, we can conclude that the reverse realization type must change at l_0 . Namely, there are two pairs of collinear bars in $G(p)$, one corresponds to the k^{th} forward construction step, the other corresponds to the change in the reverse realization type. However this violates our assumption of genericity of linkages that at most two bars can be collinear in any realization. \square

Proof of Lemma 5 (change of realization type). Suppose the linkage changes forward realization type at $l_f = l_0$ during the continuous motion. In other words, the linkage realization has forward realization type σ immediately before reaching l_0 , and has forward realization type τ immediately after reaching l_0 , where $\sigma \neq \tau$. To guarantee continuous motion, the forward realization type at l_0 must be compatible with both σ and τ . Due to the genericity assumption

on linkages, this is possible only if σ and τ differ at exactly one entry which is 0 at l_0 . Therefore the realization at l_0 is a realization of an extreme linkage. By Lemma 4 (ii), l_0 must be an interval endpoint of both $\Phi_f(G, \bar{l}, \sigma)$ and $\Phi_f(G, \bar{l}, \tau)$. \square

F Details of the complete Cayley vector

F.1 Definition of minimal complete Cayley vector for general 1-dof graphs of low Cayley complexity

Given a general 1-dof tree-decomposable linkage (G, \bar{l}) with low Cayley complexity on base non-edge $f = (v_0, v'_0)$, we define a minimal *complete Cayley vector* F using the following iterative procedure of adding edges to G until it becomes triconnected and redundantly rigid (i.e. globally rigid).

(1) Add the edge (v_0, v'_0) to G , and call the obtained graph G^+ . As long as (v_0, v'_0) remains a two-separator of G^+ , we take two arbitrary vertices v_k and v'_k , which are in the last level of G and are separated by (v_0, v'_0) in G^+ , and add the edge (v_k, v'_k) to G^+ .

(2) While there are remaining vertices in the last level of G^+ , we repeat the following. (a) If there are two or more vertices in the last level of G^+ , we take an arbitrary pair from them and add an edge between. (b) If there is only one vertex v_k in the last level of G^+ , we add one of the following three edges to G^+ : (i) the edge $e_1 = (v_0, v_k)$, if (v_0, v_k) is a non-edge in G ; (ii) the edge $e_2 = (v'_0, v_k)$, if e_1 is not added and (v'_0, v_k) is a non-edge in G ; (iii) the edge $e_3 = (v_k, v'_k)$ where v'_k is any vertex in last level vertex in G different from v_k , if neither e_1 nor e_2 is added.

(3) While G^+ is not 3-connected, we repeat the following. Take any two separator (v_m, v_n) of G^+ . Take any last level vertex v_k of G that cannot be constructed from f in G without constructing both v_m and v_n . If (v_0, v_k) is a non-edge, we add the edge (v_k, v_0) to G^+ , otherwise we add the edge (v'_0, v_k) to G^+ .

The minimal complete Cayley vector F consists of all the edges we added in this procedure above.

F.2 Proofs of global rigidity

Proof of Lemma 6 (1-path global rigidity). The 3-connectivity is clear to verify.

For redundant rigidity, we use G^+ to denote the graph obtained by adding the non-edges in the complete Cayley vector as edges to G . Without loss of generality, assume the edges added are (v_0, v'_0) and (v_0, v_n) . For contradiction, assume that after removing an edge (x, y) from G^+ , the remaining graph G' is not rigid. Clearly (x, y) is not the edge (v_n, v_0) .

Since we assume that each cluster of G is globally rigid, here we only consider the case that (x, y) is not in any non-trivial cluster of G .

Since G' is not rigid and G' satisfies $|E'| = 2|V'| - 3$, there must exist a subgraph G_S of G with $|E_S| > 2|V_S| - 3$. The subgraph G_S must also contain the edge (v_n, v_0) , since the tree-decomposable graph $G \cup f$ is minimally rigid thus cannot contain a subgraph satisfying such a condition.

So $G_S = G_f \cup (v_n, v_0)$, where G_f , having $|E_f| = 2|V_f| - 3$, is a minimally rigid subgraph of the tree-decomposable graph $G \cup f$, and contains both v_0 and v_n . We have the following cases:

(a) G_f is a single edge, that is (v_n, v_0) . This contradicts our construction of the complete Cayley vector that (v_0, v_n) should be a non-edge of G .

(b) G_f is a cluster that is not reduced to an edge. Since G_f contains v_n and v_n is a last level vertex, this contradicts our assumption that each cluster not reduced to an edge has at least 3 shared vertices with the rest of the graph.

(c) G_f contains the edge (v_0, v'_0) , and does not contain both x and y . Since G_f contains v_n , there exists a construction sequence from (v_0, v'_0) to v_n . So v_n can be constructed in G from (v_0, v'_0) without first constructing both x and y , contradicting the 1-path property of G . \square

Proof of Lemma 7 (multi-path global rigidity) . The 3-connectivity is clear from the construction.

For redundant rigidity, we use G^+ to denote the graph obtained by adding the non-edges in the complete Cayley vector as edges to G . For contradiction, assume that after removing an edge (x, y) from G^+ , the remaining graph G' is not rigid. Clearly $(x, y) \notin F \setminus f$.

Let v_k be any last level vertex in G which depends on (x, y) , namely v_k cannot be constructed from f without constructing both x and y (here v_k can be any last level vertex if $(x, y) = f$). We have the following cases:

(1) The graph G^+ contains the edge (v_0, v_k) (or (v'_0, v_k)).

Starting from $G \cup f$, we remove all last level construction steps, till v_k becomes the only last level vertex in the remaining graph P (other than possibly v_0 and v'_0). Let $P^+ = P \cup (v_k, v_0)$.

P is a 1-path tree-decomposable graph with base edge f . By Lemma 6, $P^+ \setminus (x, y)$ is rigid. So $G^+ \setminus (x, y)$ is also rigid, since adding back the construction steps preserves rigidity.

(2) The graph G^+ does not contain the edge (v_0, v_k) or (v'_0, v_k) . So there must be another last level vertex v_j of G , such that G^+ contains the edge (v_j, v_k) .

Starting from $G \cup f$, we remove all last level construction steps, till v_k and v_j become the only last level vertices in the remaining graph P (other than possibly v_0 and v'_0). Let $P^+ = P \cup (v_j, v_k)$. We can use an argument similar to the proof of Lemma 6 to prove the rigidity of P^+ . \square